ESD-TR-70-303

MTR-1779

PRELIMINARY REPORT ON THE DISCRETE CLUTTER MEASUREMENT PROGRAM

E. P. McCurley

W. J. McEvoy

SEPTEMBER 1970

Prepared for

DEPUTY FOR AIRBORNE WARNING AND CONTROL SYSTEMS
ELECTRONIC SYSTEMS DIVISION
AIR FORCE SYSTEMS COMMAND
UNITED STATES AIR FORCE
L. G. Hanscom Field, Bedford, Massachusetts

Project 4110

Prepared by
THE MITRE CORPORATION
Bedford, Massachusetts

Contract F19(628)-68-C-0365

ESD-TR-70-303

MTR-1779

PRELIMINARY REPORT ON THE DISCRETE CLUTTER MEASUREMENT PROGRAM

E. P. McCurley

W. J. McEvoy

SEPTEMBER 1970

Prepared for

DEPUTY FOR AIRBORNE WARNING AND CONTROL SYSTEMS
ELECTRONIC SYSTEMS DIVISION
AIR FORCE SYSTEMS COMMAND
UNITED STATES AIR FORCE
L. G. Hanscom Field, Bedford, Massachusetts

Project 4110

Prepared by
THE MITRE CORPORATION
Bedford, Massachusetts

Contract F19(628)-68-C-0365

FOREWORD

This report has been prepared by The MITRE Corporation under Project 4110 of Contract F19(628)-68-C-0365. The contract is sponsored by the Electronic Systems Division, Air Force Systems Command, L. G. Hanscom Field, Bedford, Massachusetts.

REVIEW AND APPROVAL

Publication of this technical report does not constitute Air Force approval of the report's findings or conclusions. It is published only for the exchange and stimulation of ideas.

KENDALL RUSSELL, Colonel, USAF
Deputy for Airborne Warning
and Control Systems

ABSTRACT

As part of an experimental investigation of ground clutter being conducted by the MITRE Corporation, data on the magnitudes and distribution of large "discrete" clutter returns have been collected using a radar situated at the Boston Hill field station in North Andover, Massachusetts. Although the experiment is limited in scope and the instrumentation unsophisticated, the measurement program has confirmed some earlier ideas about discrete land clutter, and suggests other promising lines of experimentation. The objectives of this report are to (a) describe the instrumentation, measurement methods, and physical environment, (b) make available the measured results obtained thus far, and (c) provide the background for future effort.

ACKNOWLEDGMENT

The writers wish to thank E. W. Beasley, R. W. Jacobus, and L. P. Shepherd for helpful discussions and suggestions. In addition, the writers are indebted to M. J. Gunn and T. M. Nichols for their assistance in conducting the experimental work.

TABLE OF CONTENTS

LIST OF ILLUSTRATIONS

LIST OF ILLUSTRATIONS (CONCLUDED)

LIST OF TABLES

SECTION I

INTRODUCTION

A. Discussion of Discrete Clutter

A major consideration in the design of an airborne search radar for overland operation is the radar's ability to reject ground clutter. Clearly, effective design requires detailed, accurate knowledge of clutter characteristics. Some effort has been expended in the past to collect and analyze clutter data in order to formulate useable clutter models, but not nearly enough to satisfy the needs. Attempts to provide universally acceptable models are hindered by a lack of agreement about the dominant mechanisms involved. In practice, the models utilized considered the clutter return to result from the contributions of a number of independent random scatterers distributed over the ground (or comprising the ground). The equivalent radar cross section then is proportional to the total number of such scatterers illuminated by the antenna with appropriate weighting for the antenna gain function. (However, numerical values for model parameters have been in dispute.) Lately, there has been increasing attention paid by workers concerned with AWACS performance to the expansion of the ground clutter model to include "discrete" clutter. The work reported here was motivated by concern over the potentially detrimental effects of discretes on AWACS radar performance. It is expected that the data gathered will

also be applicable to other surveillance problems, not necessarily airborne, where ground clutter is a design consideration.

The origin of the term "discrete" is unknown to the writers. Moreover, a definition complete and precise enough to earn wide acceptance might be difficult to construct at this time. It should be sufficient to note that a discrete is taken to be a highly localized scatterer, sufficiently large in radar cross section to be distinguished from the general clutter background. Such man-made objects as radio towers, bridges, and railroads would be expected to create discretes, while natural objects such as steep mountain sides, or the fortuitous combination of many returns from a forest are also possible sources. Observations of discretes suggest that they exhibit much less fluctuation than the general clutter background, but this remains to be established in fact.

Generally speaking, the impact of discrete clutter on radar design varies in detail depending on the basic radar technique employed, such as low or high PRF, and on the nature of peripheral devices that may be employed, such as main-beam blankers. The tolerance of a surveillance system to the false alarms generated by discretes will depend on the degree of sophistication of the data processor and tracking algorithms. The problem common to all systems is that a discrete of sufficiently large amplitude may be acquired by the radar antenna sidelobes. For an airborne radar

using clutter rejection techniques based upon the doppler principle, the particular problem arising is that a discrete detected in the sidelobes will have a range rate not equal to that of main beam clutter and will not be rejected.

Thus, at the input to the receiver a discrete can have the appearance of a target of interest. The manner in which range dependence becomes a consideration depends upon the choice of radar technique. The severity (or even existence) of the problem in any given application is therefore determined primarily from a knowledge of peak antenna sidelobes as well as the parameters of the discrete model. Antenna patterns of the candidate AWACS radars are now reasonably well documented, but an almost total absence of experimental data prevents the use of other than a hypothetical model for discretes. In fact the existence of discretes has been questioned, although experiences with the APS-111 (XN-1) have argued most persuasively for their existence and importance to a complete clutter model. Recent analyses conducted by both AWACS radar candidates have indicated that, even at the relatively low sidelobe levels currently being achieved, large discretes may present a considerable problem. Unfortunately, the experimental work conducted so far in the AWACS program has not provided the necessary data for evaluating the severity of the problem.

Specifically, in order to formulate an experimentally-based discrete clutter model, data are required to answer the following questions:

(1) What are the sources of discrete returns?

(2) What radar cross sections do they present?

(3) How many discretes may be expected in a given area, and how are they distributed?

(4) What are the fluctuation characteristics of discretes?

To provide some further information about discretes that will be of value in the design and evaluation of AWACS radars, an S-band measurement program was devised and is currently being pursued. The experiments envisaged are of limited scope and will not answer all the questions posed above, but it is believed that where so little information now exists, the program can provide some valuable practical data. This report gives the results obtained so far, describes the equipment, measuring procedures, and region under investigation, and also provides a basis for future activity.

B. Review of Relevant Background

The general trend in the characterization of clutter has been to fit measured data to "clutter models" in which the returns from a patch of terrain illuminated by a radar have a mean value proportional to the reflectivity, σ^o, and some probability distribution, such as Rayleigh. The models include, in general, dependence

on various parameters such as grazing angle, polarization, wind velocity, and so on. With few exceptions, there has been no special recognition that, embedded in the clutter patch seen by a radar, there may be one or more steady reflectors large enough to dominate or materially increase the clutter return over that from the terrain itself. No doubt many observations have been made with operational and experimental radars of persistent returns from a given area. Nevertheless, apparently little systematic attention has been directed toward the study of this discrete effect. In the discussion below the exceptions will be noted.

Apparently, the first references to discretes, though somewhat oblique, are by Kerr[1], and Lawson and Uhlenbeck[2]. Kerr recognizes that man-made objects as well as rocks and tree trunks may cause a large, steady component of returned power. A model, referred to as "random scatterers plus a steady signal," is discussed in both references. Experimental investigations and the application of results by Kerr were confined to terrain where (implicitly) there were no discretes[3]. In the discussion of atmospheric effects Kerr refers in several places to the use of standpipes for reference targets. Interestingly enough, he concludes that variations in propagation conditions cause the apparent cross section to vary widely[4].

In 1968, Reiss et al[5] reported the results of C-band clutter measurements made on terrain characterized as rural (southern England). The clutter returns of certain cells were due in part to buildings and pylons (towers supporting power lines). Sweep-by-sweep amplitude measurements were made on clutter patches containing the discretes, and the data were fitted to the "random scatterers plus a steady signal" model developed in Kerr (referred to as a Rice distribution by the authors). Two pylons had respective cross sections of 29 m^2 and 220 m^2. The difference is attributed to the fact that these directive reflectors were viewed from different angles. Slow variations of the mean cross section with time were observed, and these were tentatively attributed to changes in atmospheric conditions affecting propagation. Such an interpretation is consistent with observations made by Kerr in experiments on one-way transmission. A short decorrelation time for the larger pylon was attributed to the decorrelation of the background clutter.

In 1960, Edison et al[6] reported the results of clutter measurements at high grazing angles (60°-90°). The approach was to resolve clutter returns into specular and scattered components. It was observed that some targets gave a highly specular return characterized by a very small range of fading, and a returned pulse of the same width as the transmitted pulse. No details are given as to the sources of these specular returns, but it is possible that the returns were from discretes.

The recent interest in discretes vis-à-vis airborne search radar is reflected by Carlson and Greenstein[7]. They acknowledge that there is a scarcity of data, and postulate a statistical model for use in assessing the vulnerability of AWACS radars to discretes. In a discussion of discrete clutter characteristics, Carlson and Greenstein adopt the viewpoint that, among other things, discrete clutter fluctuates at a "lower rate" in contrast to the view that it exhibits little, if any, fluctuation[8]. Perhaps, however, it might be either in any given measurement scheme. If, for example, the discrete is a highly directive reflector, then in an airborne situation the aircraft motion could produce an apparent fluctuation. Similarly, if the discrete were not extremely large relative to a fluctuating background, then fluctuations could be observed.

Hemenway et al[9] are the only known clutter investigators specifically concerned with discrete clutter measurements made from an airborne radar. A limited series of test flights was conducted over New Jersey. The presence of discretes was confirmed, and cross sections as large as 10^6 m^2 were measured at UHF. The smaller discretes fluctuated more than the larger.

C. Basic Measurement Technique

The method of measurement is best described by reference to the radar range equation as given in Kerr[10]:

$$S = \frac{PG^2 \sigma \lambda^2}{(4\pi)^3 R^4} F^4 \qquad (1)$$

In Equation (1) S is the received power from a target of cross section σ at range R, when the peak transmitted power is P. Here G is the effective free-space antenna gain at the peak of the antenna beam, F is the pattern propagation factor, and λ is the wavelength. To underline the importance of F, its definition is quoted from Kerr:

> "The pattern propagation factor F is defined as the ratio of the amplitude of the electric field at a given point under specified conditions to the amplitude of the electric field under free space conditions with the beam of the transmitter directed toward the point in question. In symbols,
>
> $$F \equiv \left| \frac{E}{E_o} \right|, \qquad (2)$$
>
> where... E_o is the magnitude of the free space field at a given point with the transmitting antenna oriented directly toward the point and E is the field to be investigated at the same point."

Under free-space conditions F expresses the antenna pattern function. In the presence of the earth it involves, additionally, the effects of interference (multipath), diffraction, and refraction.

The measurement technique utilized consisted in measuring S,P,G, and R. Substituting these quantities in Equation (1) yields a measurement of the product σF^4. Since it is virtually impossible to measure F (except under very specific conditions), we then define σ_e as the measured cross section of discretes, where

$$\sigma_e \equiv \sigma F^4. \tag{3}$$

In the discussion of measured discrete cross section, it should be recognized that σ_e is the quantity to which reference is being made. Figure 1 is a plot of S versus R for several values of σ_e, using measured values of transmitter power, P, and antenna gain, G.

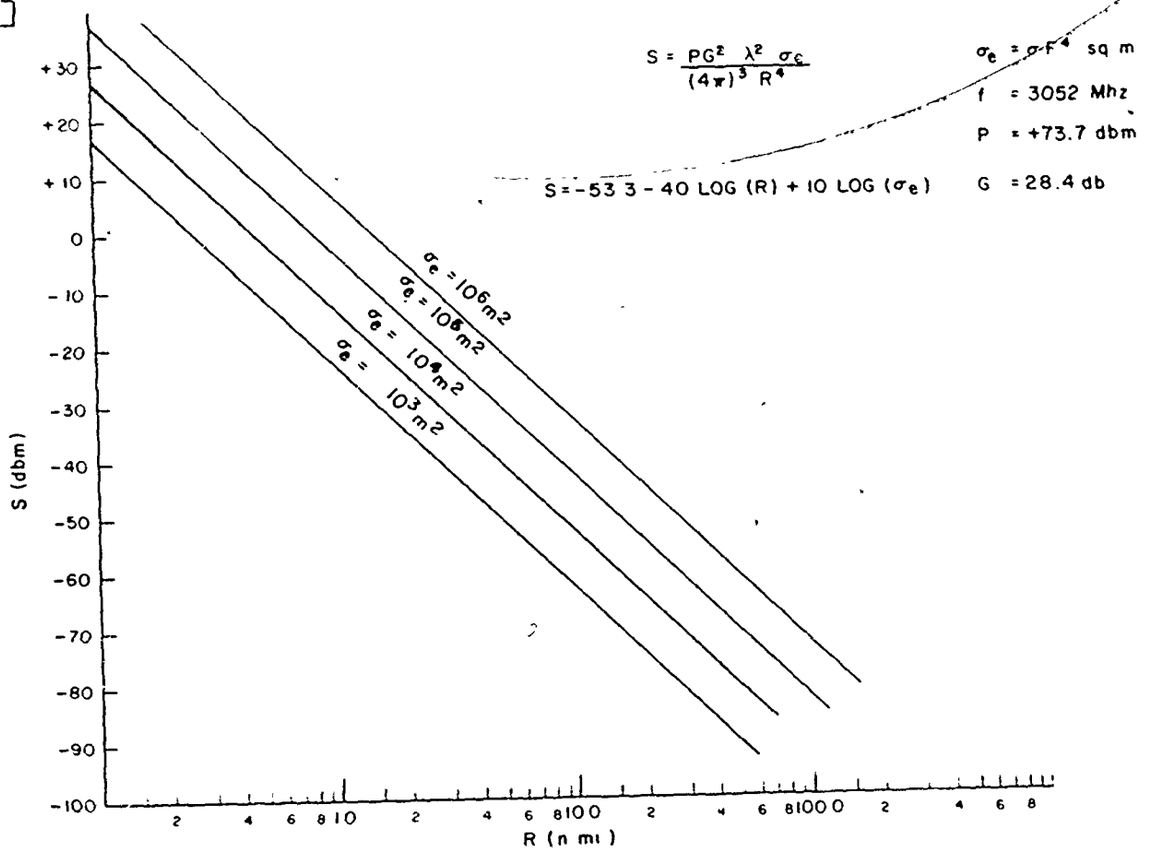

Figure 1 RECEIVED SIGNAL POWER vs. RANGE FOR VARIOUS RADAR CROSS SECTIONS (BASED UPON MEASURED RADAR PARAMETERS)

SECTION II

EXPERIMENTAL PROCEDURE

A. General Considerations

The anticipated characteristics of discrete clutter suggested that the measurement instrumentation could be relatively simple, and that the design of the experiment could be based on the following major considerations:

(1) The sizes of discretes of primary interest, thousands of square meters, would permit utilization of a low-power radar.

(2) Extremely accurate absolute measurement of discrete cross section was judged to be of secondary importance; order-of-magnitude values for the cross sections would be sufficient to define the discrete phenomenon. In actual fact, propagation effects limit the precision of the cross section measurement.

(3) The number of discretes in the region to be investigated was assumed to be sufficiently small so that elaborate automatic data recording and analysis would not be required.

(4) Similarly, a lack of significant sweep-to-sweep fluctuation would obviate the necessity for compiling detailed statistics on any given discrete by means of automatic data recording and analysis. Experience showed this to be quite true of the larger discretes (discretes greater than 10^4 m^2), but less true of the smaller (between 10^3 and 10^4 m^2).

(5) The spatial distribution of discretes could be displayed conveniently on an ordinary Plan Position Indicator (PPI). By introducing suitable thresholds, then cross section versus spatial distribution could also be obtained economically.

In order to identify the sources of discrete returns, somewhat more detailed measurements and procedures were required. These were feasible for only the largest discretes observed, which are arbitrarily taken to be 10^4 m^2 or greater. The actual procedure used to identify discretes is described below in Section II-E.

B. Description of the Radar

The radar utilized in the measurement program is a non-coherent S-band marine radar, type CRM-N2C-30, manufactured by Radio Corporation of America. The three basic components are the transmitter/receiver group, the antenna including the drive system and rotary joint, and PPI indicator. The system block diagram is shown in Figure 2.

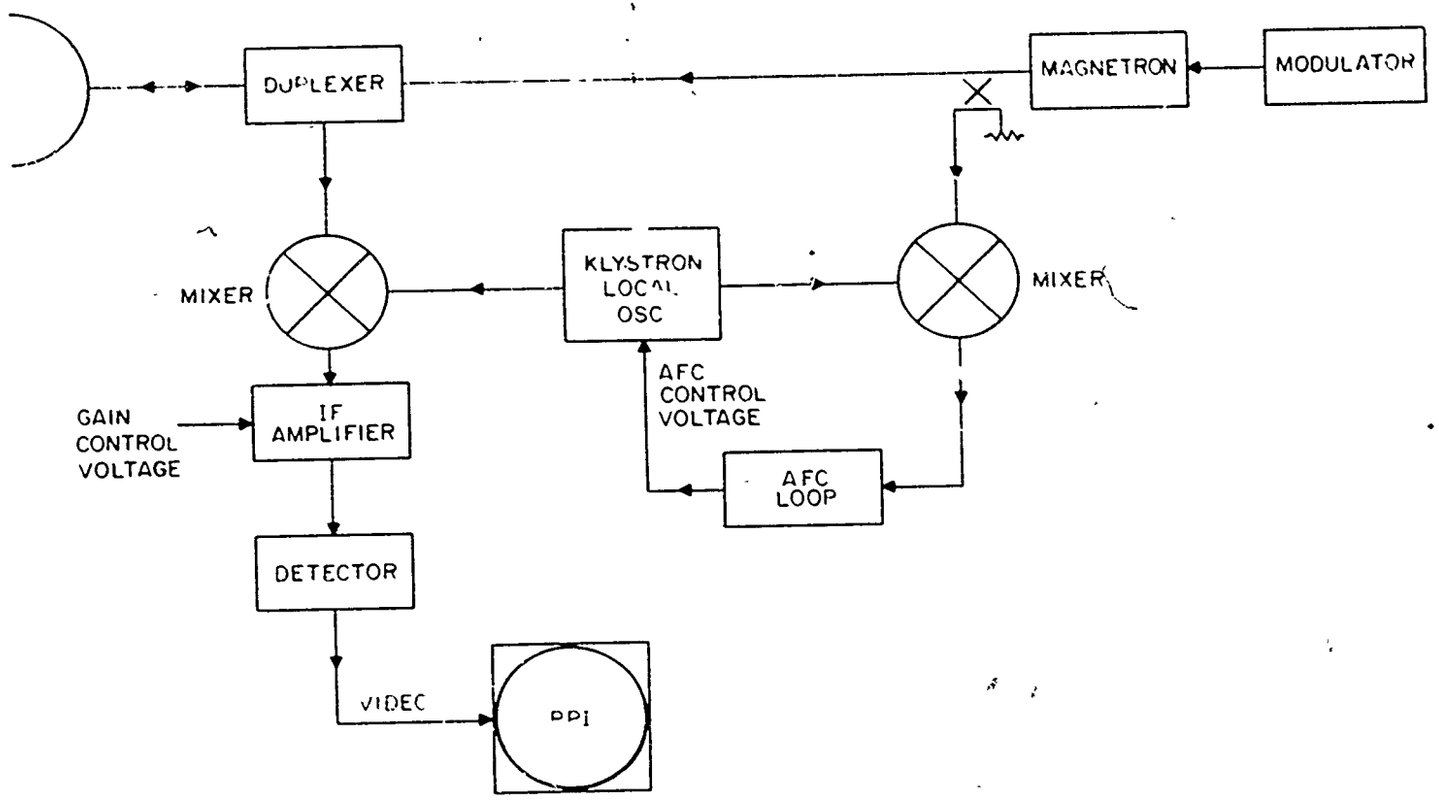

Figure 2 SIMPLIFIED RADAR BLOCK DIAGRAM

The major radar parameters are:

Frequency:	3052 Mhz
Peak Power:	23.5 Kw*
Pulse Length:	0.4μsec** (Range Resolution: 200 ft)
Pulse Repetition Rate:	1 Khz **
Antenna:	
Polarization -	Horizontal
Vertical Beamwidth -	20 degrees
Horizontal Beamdwidth -	2 degrees
Gain -	28.4 db*
Side Lobes -	28 db, one-way (max)
Rotation Rate -	Variable to 13 r.p.m.
I.F. Amplifier:	
Type -	Linear, with voltage-controlled gain
Center Frequency -	30 Mhz
Bandwidth -	3 Mhz **

*See Figure 3 for definition of reference planes.

**The radar has an alternate mode with a 0.1-μ sec pulse width and a 2-Khz repetition rate which was not utilized in the experiment.

C. Radar Calibration

A block diagram useful for the discussion of radar calibration is shown in Figure 3. Essentially, the antenna gain was measured at the input to the rotary joint; then the insertion loss of the waveguide run between the transmitter and the antenna was measured and subtracted from the antenna gain, thus referring the antenna gain to the plane where the peak power was measured and test signals were injected.

Transmission Line Loss

Standard voltage standing wave ratio techniques were utilized for the measurement of the low value of insertion loss of the waveguide run. The measured insertion loss had a one-way value of 0.84 db. This value is in good agreement with calculations based upon published data for the waveguide loss.

Peak Power

The peak power was measured by comparing (on an A-scope display) the detected amplitudes of an attenuated sample of the transmitted pulse and a test pulse. The attenuation required for equality plus the measured power of the test pulse gave the transmitted power. Values ranging from + 73.5 to + 73.7 dbm were measured. The value of + 73.7 (23.5 kw) was taken to be the

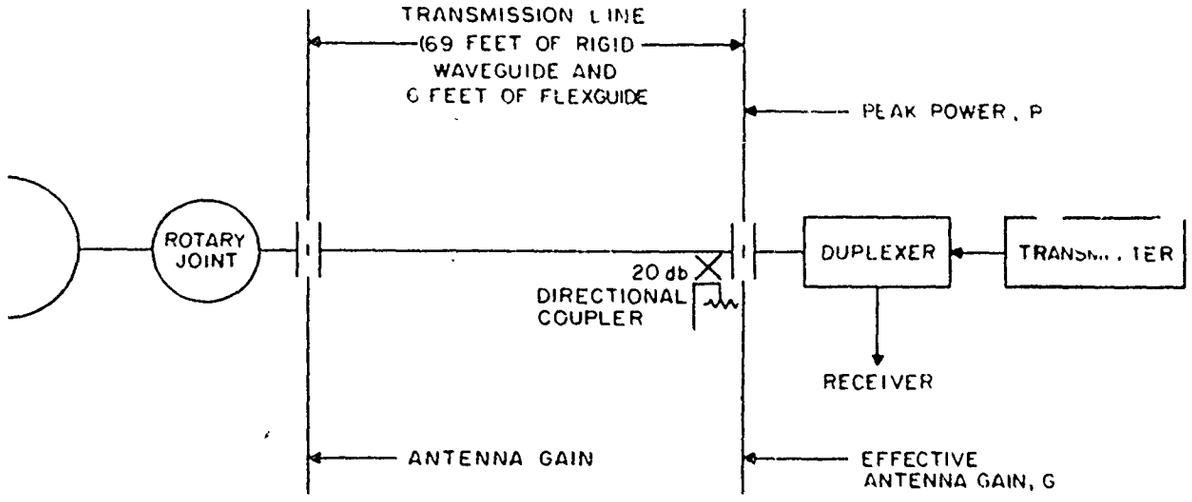

Figure 3 BLOCK DIAGRAM SHOWING REFERENCE PLANES FOR RADAR PARAMETERS

transmitted power. Making allowances for the fact that the measurement includes duplexer loss, this value is in good agreement with the radar manufacturer's claim of 30 KW or + 74.8 dbm.

Antenna Gain

Antenna gain was measured by a substitution method using a standard gain horn. A source was located at Mills Hill, approximately 1.5 n.mi. from Boston Hill. A received power measurement was made with the standard gain horn (18.1-db gain) and then repeated with the radar antenna, with attenuation added to yield equal power outputs in both cases. In principle the gain of the radar antenna then equalled the attenuation plus the gain of the standard gain horn.

Some difficulty was encountered in measuring the actual antenna gain. It was observed that the field incident upon the aperture was not uniform, as determined by probing the field systematically across the face of the aperture. Therefore, a series of gain measurements was made and averaged. The gain measurements, made along the vertical center line of the aperture, averaged 29.25 db. This value is in good agreement with values measured by the antenna manufacturer when allowance is made for rotary joint losses.

The effective antenna gain as used in the range equation was taken as the antenna gain less the transmission line loss, or 28.4 db.

D. Measurement Instrumentation

Measurement System

A simplified block diagram showing the radar and accessory test equipment during operation is given in Figure 4. Figures 5 and 6 are photographs of the antenna and the system, respectively. Three sections of the measurement setup are defined in order to facilitate discussion. Briefly, the radar was modified to provide a constant video output for a target of given cross section, independent of range, from one mile to approximately thirty-seven nautical miles. This was achieved by increasing the IF gain as a function of range so that the R^{-4} dependence of the target was removed. This was accomplished by application of a "sensitivity time control" (STC) voltage to the IF amplifier bias circuit. The video voltage corresponding to a target was then compared with a reference voltage in a threshold comparator, and the output displayed in several formats.

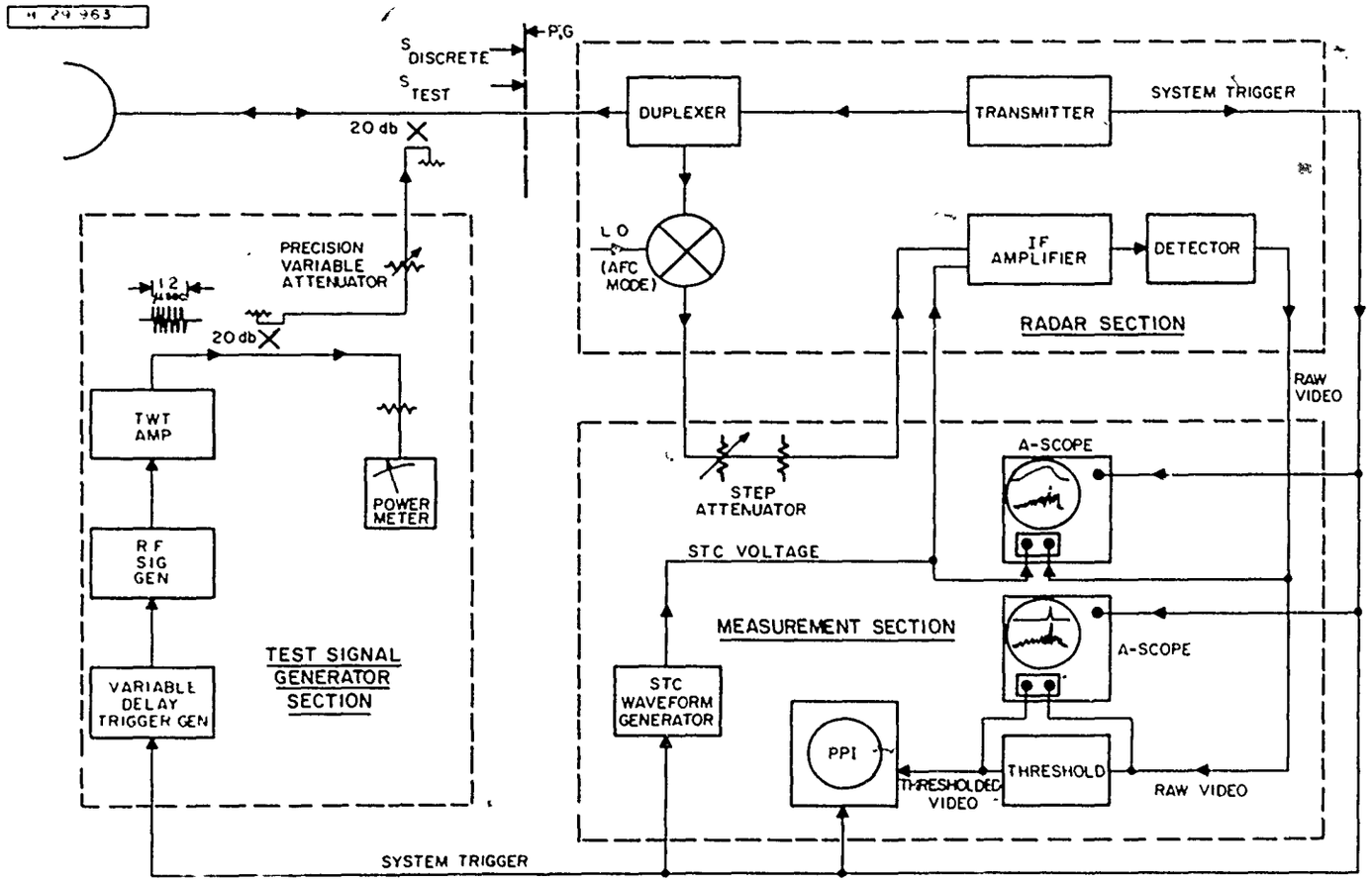

Figure 4 INSTRUMENTATION SYSTEM BLOCK DIAGRAM

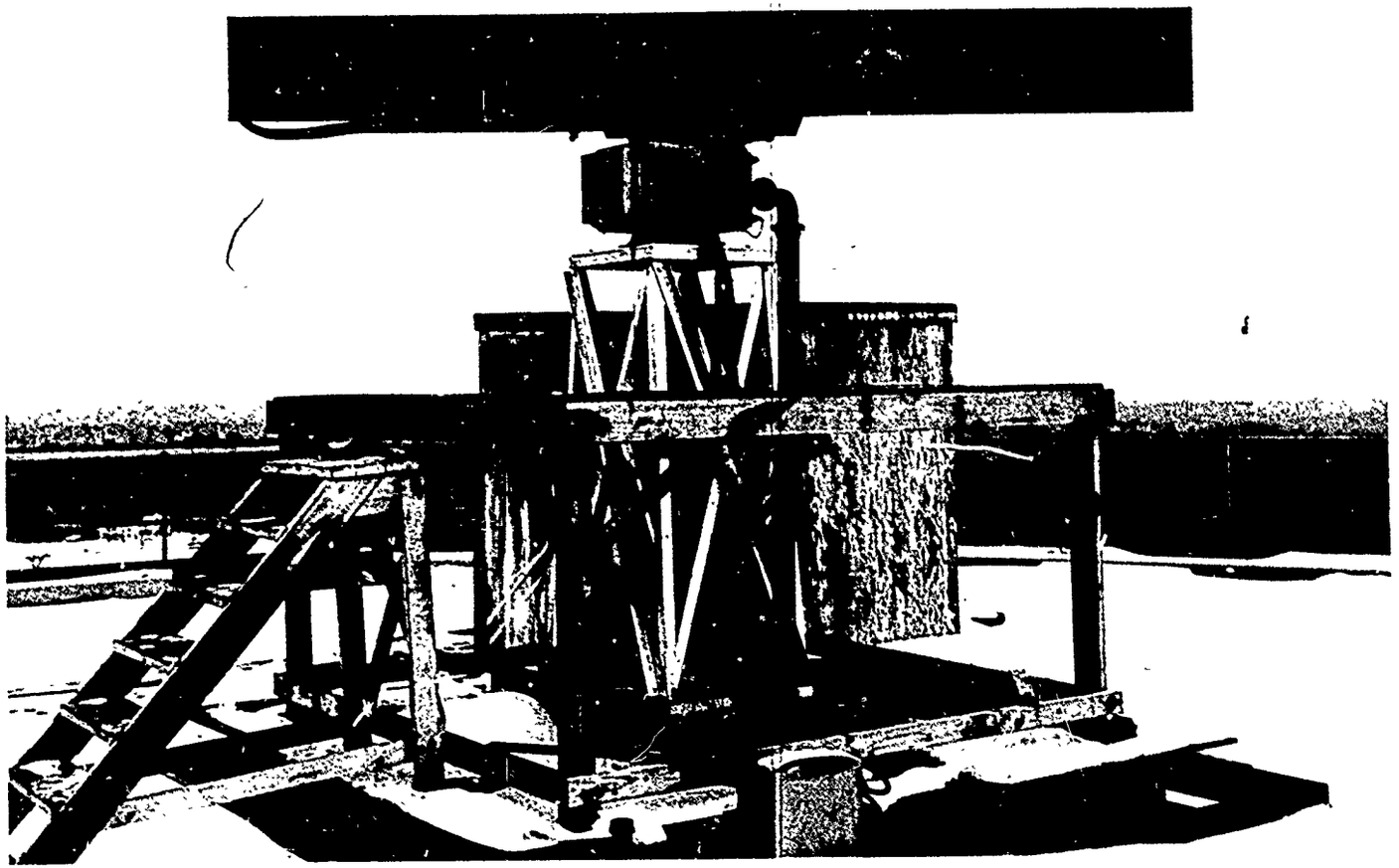

Figure 5 View of Antenna

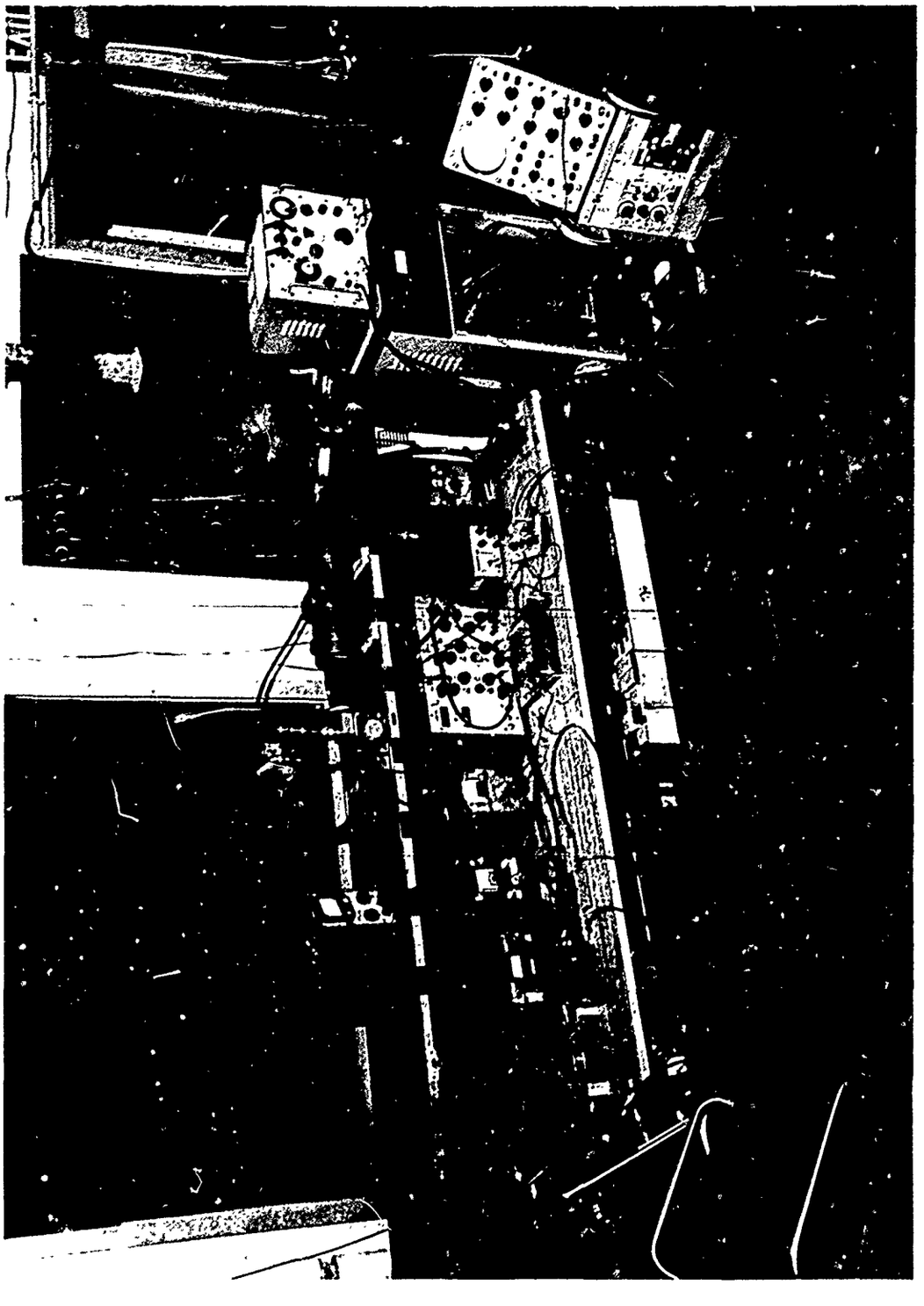

Figure 6 View of System

Test Signal Generator Section

The test signal generator section provided for the injection of a signal of known power at any range of interest into the radar for the purposes of either comparison with the return from a discrete or the calibration of the STC waveform. The signal was injected into the radar by means of a 20-db directional coupler located at the plane where antenna gain and peak transmitted power were measured. In order to vary the range of the test signal, the system trigger was delayed by means of the variable delay trigger generator and applied as a trigger to the RF signal generator which, utilizing internal modulation, generated a 1.2-microsecond pulse at the system frequency (3052 Mhz). The selection of 1.2 microseconds was based upon the need for a pulse as wide as possible relative to the transmitted pulse (in this case three times as wide) to assure that the pulse spectrum fell within the IF passband. On the other hand, the pulse width had to be short enough to be substantially unaffected by the range-variable gain of the IF amplifier when the test pulse was used for comparison with the return from a discrete at a given range. A TWT amplifier followed the signal generator and served a two-fold purpose. By operating in saturation, power-level stability was assured, and the relatively high power level permitted convenient monitoring and adjustment of the test signal level. The precision variable attenuator had a 50-db range so that a 50-db dynamic range of test signals could be accurately and conveniently obtained.

Measurement Section

Three functions were performed by this section:

(a) Generation of the STC waveform

(b) Thresholding of video

(c) Display of raw and thresholded video

As stated previously, the gain of the IF amplifier was increased with increasing range in order to remove the R^{-4} dependence of the radar returns. The IF amplifier was a linear amplifier, the overall gain of which was varied by the grid bias applied to the three input stages. The STC voltage waveform was an experimentally-determined voltage which caused the gain to vary with range in the desired manner.

The STC waveform generator received the system trigger which started an astable multivibrator clock, and set the logic level of a twenty-stage clocked shift register. The output of the clock in turn was applied to the shift register, and a train of contiguous pulses was generated. The sequential output pulses of the shift register were summed in an operational amplifier and then integrated, the amplitude of each pulse being controllable. The amplitude of each pulse determined the slope at the output of the integrator for the duration of the pulse. In this way, a continuous curve was

approximated by means of linear segments. The duration of the first pulse was one mile, while the duration of each of the subsequent eighteen pulses was two miles. Integration of the first pulse caused the STC output to be the correct value at a range of one mile. Integration of the subsequent two-mile pulses generated a sufficiently accurate curve out to thirty-seven miles.

The STC waveform and a threshold reference voltage were adjusted to display only targets of a given cross section as "thresholded video". The reference voltage was set at a convenient value (approximately 0.4 volts); the video voltage then was compared with the reference in a sensitive differential comparator. When the video level was equal to or greater than the reference, a constant output voltage was generated.

RF test pulses were introduced, sequentially, into the radar at 1, 3, 5, 7,...,37 miles at power levels equivalent to the signal from a target of the specified minimum cross section as determined from Figure 1. The amplitude of the pulse from the shift register into the integrator for each range increment then was adjusted until the detected test pulse just crossed the threshold. Any discrete which was equal to or greater than the specified cross section then was amplified to a level, independent of range, sufficient to cross the threshold. With this feature the PPI displayed only the discretes above a selected cross section, regardless of their range.

Measurements were made for minimum cross sections of 10^3 m^2, 10^4 m^2 and convenient multiples thereof. In practice the procedure indicated above was employed for targets with a minimum cross section of 10^3 m^2. For cross sections of 10^4 m^2 and greater, a step attenuator and a fixed pad were inserted between the mixer and the IF amplifier. With the step attenuator set for zero insertion loss, the STC curve and reference voltage initially were adjusted to threshold on a 10^4-m^2 target. For further increases in the threshold level, appropriate attenuation was introduced by the step attenuator. The fixed pad was inserted between the mixer and the IF amplifier to reduce mismatch losses when the step attenuator was employed. This approach was not feasible for 10^3-m^2 discretes because of the degradation in the clutter-to-noise ratio. However, for returns from discretes of 10^4-m^2 cross section or greater, the noise degradation was tolerable.

E. Operational Procedure

An azimuth "ring", graduated in 0.5-degree intervals, was constructed and mounted on the antenna pedestal. A mating pointer was attached to the antenna itself. Correct orientation in azimuth was established by electrically centering the beam on the Mills Hill antenna tower, the bearing of which is accurately known relative to Boston Hill, and adjusting the pointer for this bearing. It was thereby possible to searchlight targets and obtain a more accurate azimuth than was possible with the PPI.

Additionally, a telescope was mounted on the antenna and boresighted on Mills Hill tower to aid in the identification of targets under operating conditions.

The sequence of steps involved in the measurement and identification of the discretes $\geq 10^4$ m^2 was as follows:

(1) The thresholded video was displayed for various threshold levels on the PPI and recorded photographically in order to determine the spatial distribution of discretes.

(2) The approximate range and azimuth of the discretes were determined from the PPI bearing and range cursor and recorded for reference.

(3) The discretes were then searchlighted by "hand-cranking" the antenna. By a beam-splitting process utilizing the step attenuator, the beam center was found. The azimuth was read from the azimuth ring on the anterna pedestal (estimated to 0.25 degrees). The range then was measured on an A-scope using the delayed sweep circuit. Any information regarding objects seen through the telescope was recorded, with an estimate of range.

(4) The range and azimuth determined in step (3) were converted to latitude and longitude via a set of computer-generated tables (based on the latitude and longitude of Boston Hill which are known to tenths of a second).

(5) The locations of the discretes were plotted on topographic maps (U. S. Coast and Geodetic Survey quadrangles). Water towers or other prominent objects indicated by the maps at these locations were noted.

(6) The positions where discretes were located on the maps were visited and identification made as to their nature. Water towers were confirmed at locations shown by the maps. In some cases, water towers were found where none were indicated on the map.

(7) Each discrete was searchlighted and a direct measurement made of cross section using an RF test pulse as described above. In addition, the returns were observed for fluctuation characteristics, width, and persistence.

SECTION III

DESCRIPTION OF REGION UNDER INVESTIGATION

The test radar was situated at the MITRE Boston Hill Field Station located in North Andover, Massachusetts. The elevation of the antenna was 420 feet above mean sea level; the range to the horizon, assuming a smooth earth of 4/3 true earth's radius, was 25 n.mi. (compared with the unambiguous radar range of 80 n.mi.). The region under investigation, primarily northeastern Massachusetts, is shown in Figure 7, a map of the region centered at Boston Hill. Superimposed on the map are sectors in which radar visibility was curtailed due to the close proximity of a concrete radar tower (blockage from 251 to 264 degrees true) and a platform-mounted thirty-foot parabolic antenna housed in a dielectric radome (presumed blockage from 165 to 195 degrees true).

The region under investigation is varied in character; the population centers range from small cities to rural towns, including several of Boston's suburban communities. Exclusive of the blocked sectors, there are three cities of population greater than 50,000 (part of Lawrence, one of the three cities cited, was in the

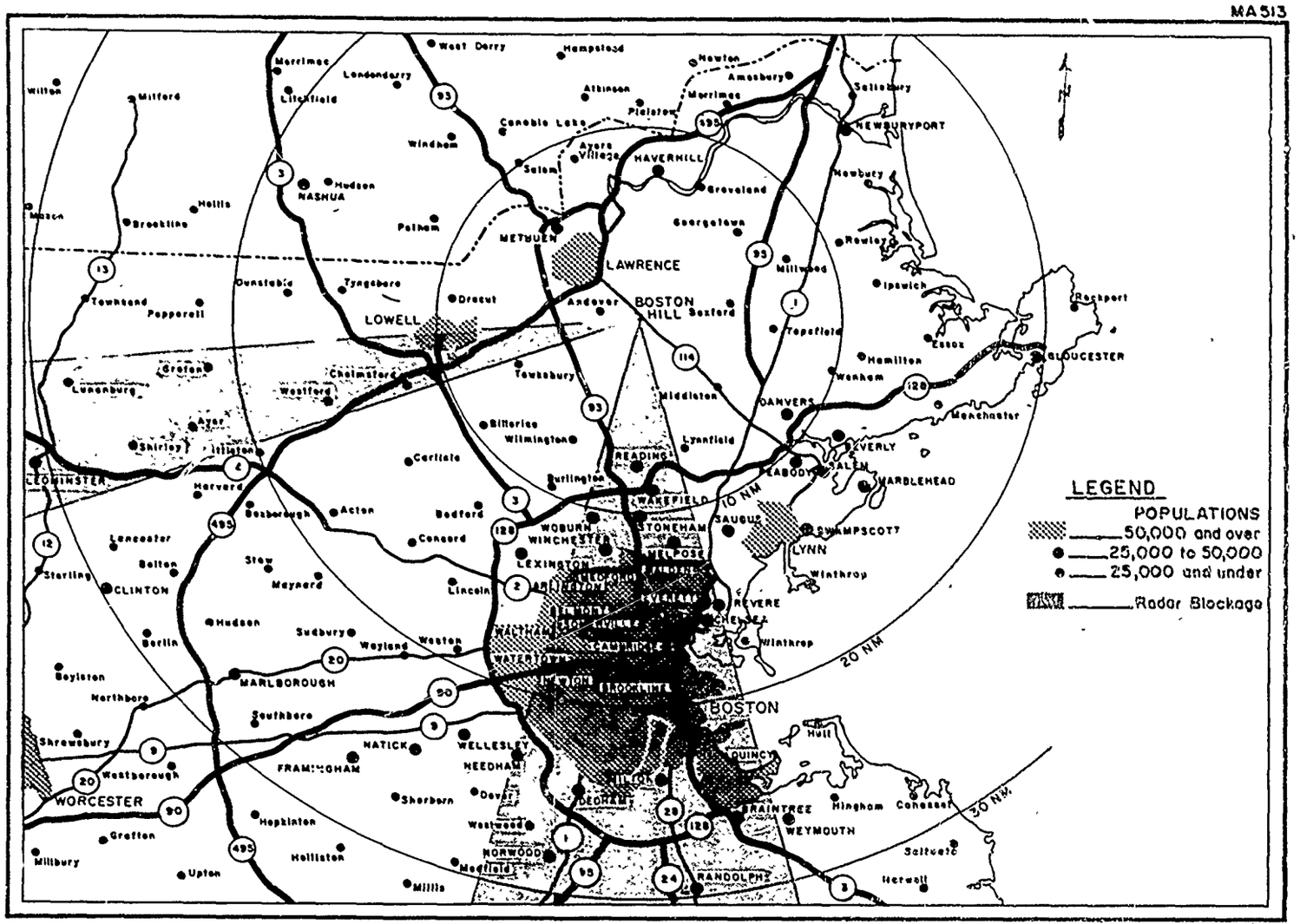

Figure 7. Map of Region Surrounding Boston Hill

blockage) and approximately twelve cities of population between 25,000 and 50,000. The general economic character of the region is light industrial. Much of the land is rural, by which is meant woodland as well as some small farms. There are many hills, and the elevation generally increases with increasing range from the west through the north. Some measure of the character of the terrain is gained by reference to Figure 8, a composite panoramic view made by mounting a camera on the antenna.

In order to determine which portions of the terrain were in shadow due to surrounding hills, a computer-generated "shadowmap" was constructed. By this technique, topographic maps of the region are subdivided into small rectangles; each rectangle is assigned an elevation equal to that of the highest point in the rectangle. The region is thereby quantized (in this case into rectangular areas). A computer program then determines for each rectangle whether its highest point can be seen from the radar, considering the heights of all intervening rectangles, and generates a map showing the visible areas. Figure 9 shows the areas visible from Boston Hill indicated by printed dots. In this way a good estimate of areas in radar shadow is obtained. Such a map cannot exactly predict the visibility of any given point, since it is based upon a topographical approximation; but general areas of visibility can be shown. It

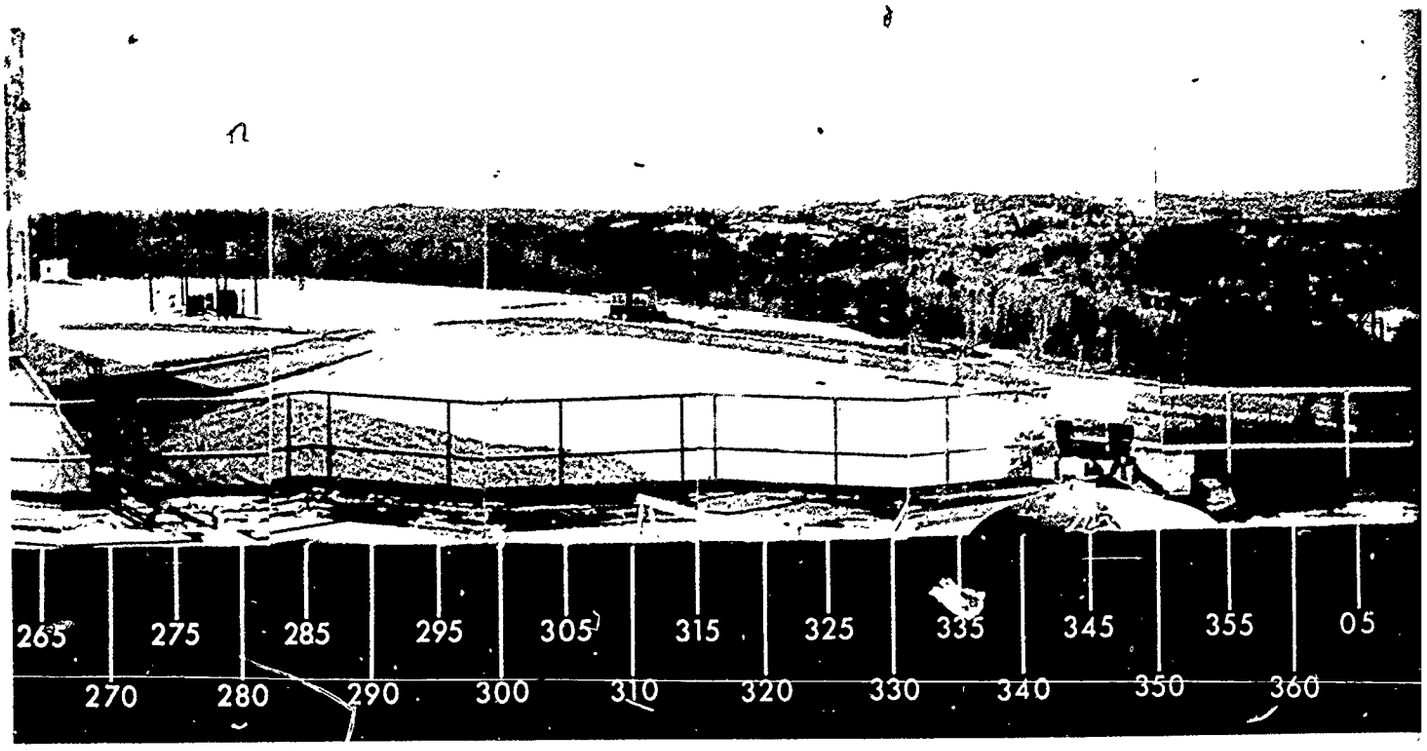

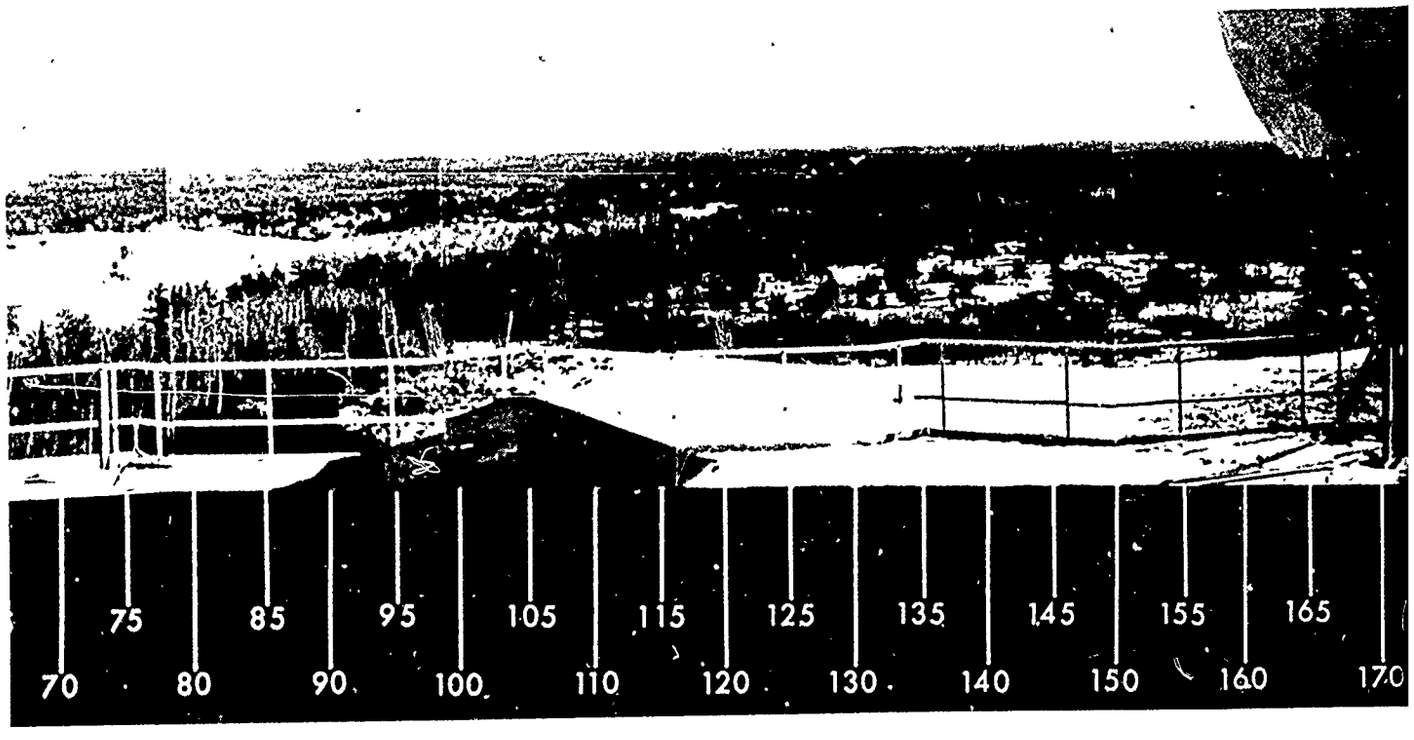

Figure 8. PANORAMIC V

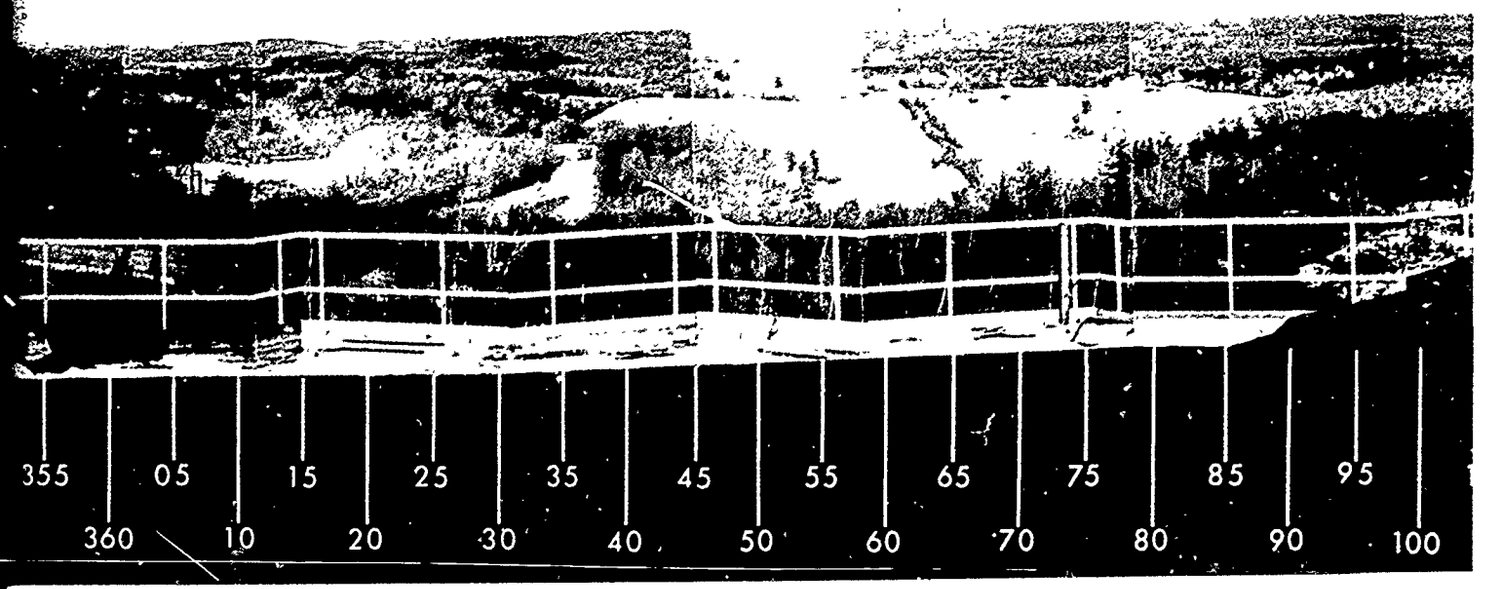

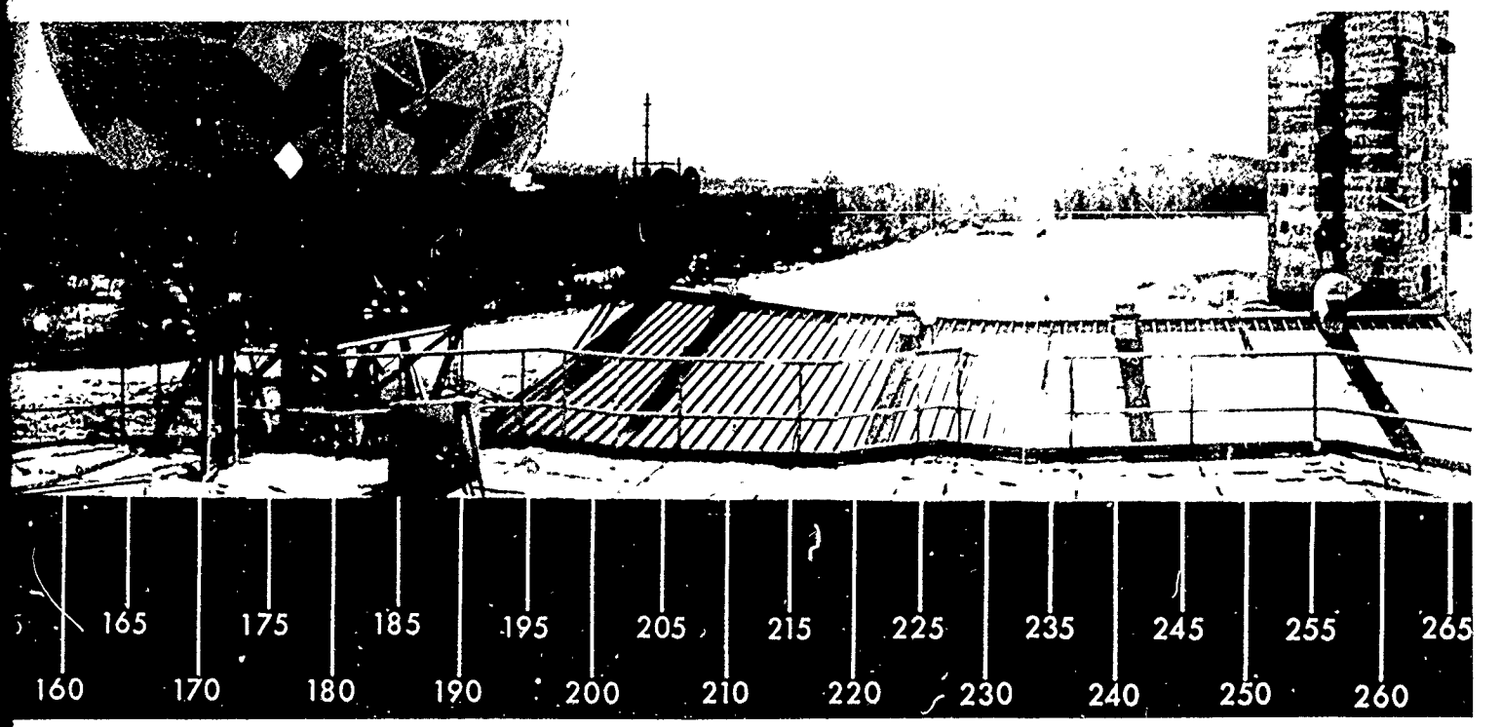

NORAMIC VIEW OF TERRAIN

B

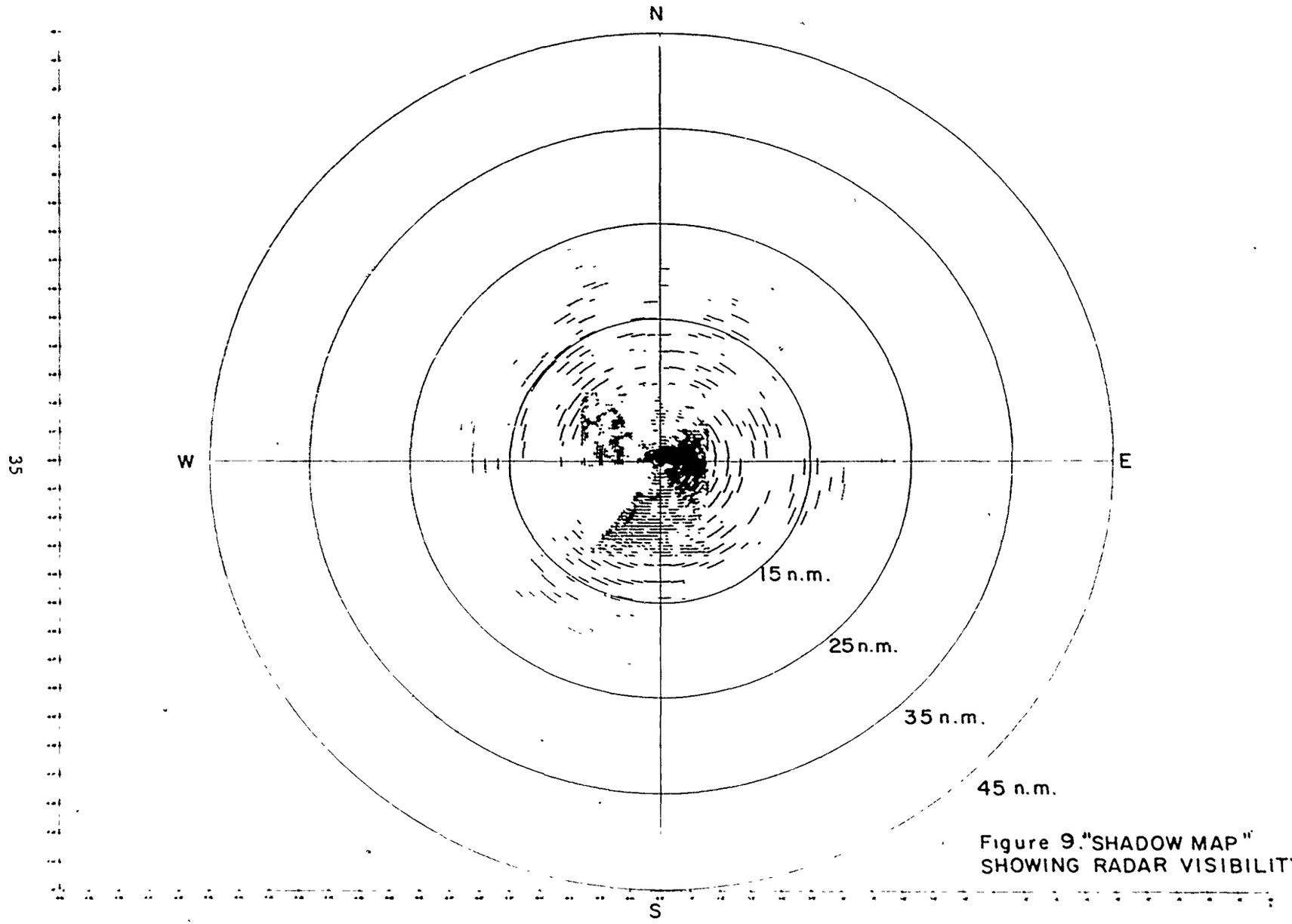

Figure 9."SHADOW MAP"
SHOWING RADAR VISIBILITY

is interesting to note the overall agreement with Figure 10, PPI photograph of the region taken without STC. The shadowmap technique is useful for selecting candidate radar sites for their visibility. Moreover, it is helpful in estimating the areal density of discretes measured from a given site.

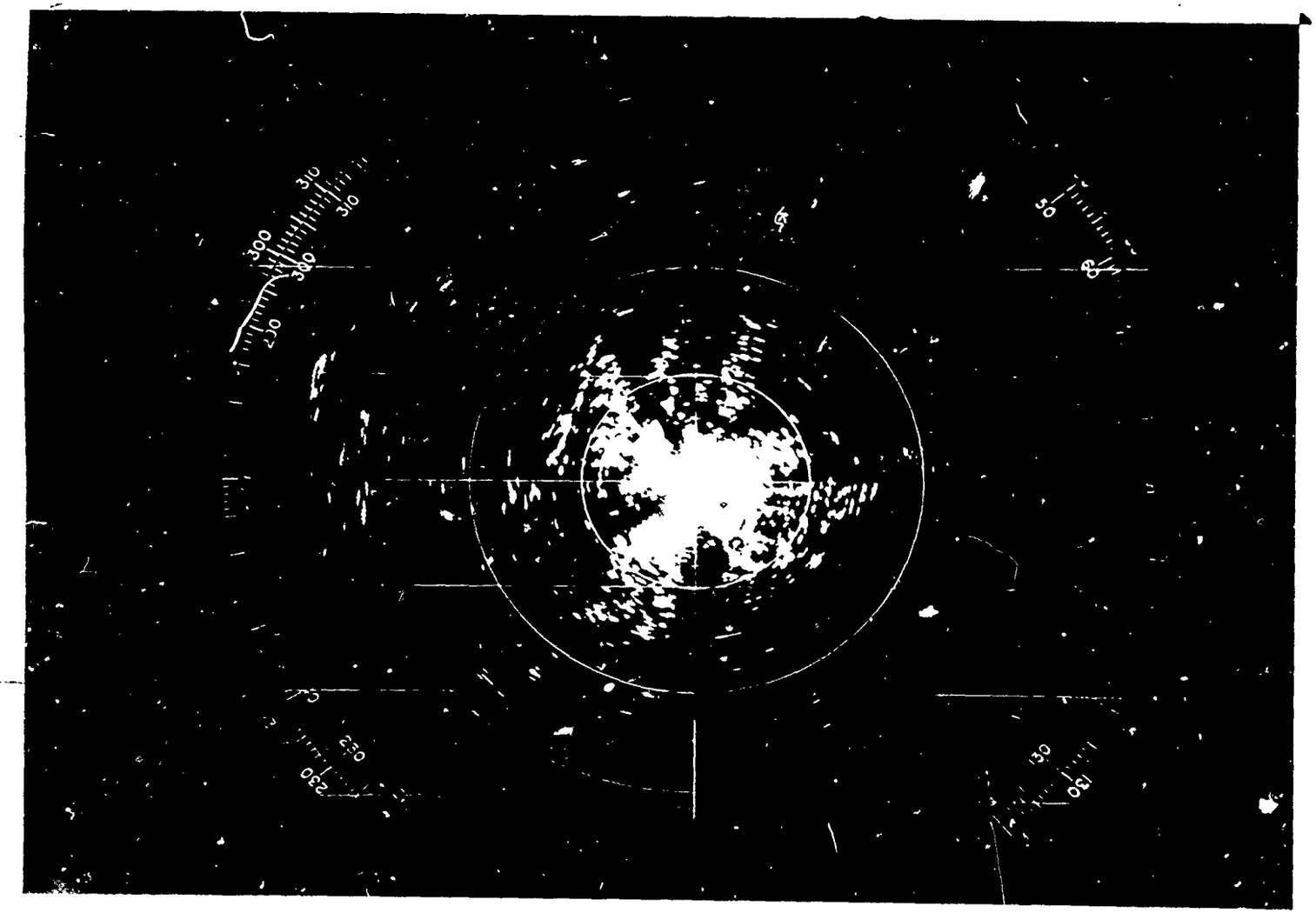

Figure 10 Clutter Map Using Raw Video (40 Mile Radial Range)

SECTION IV

EXPERIMENTAL RESULTS

A. General

Initially the STC curve and threshold were adjusted to display targets of 10^3 m^2 or greater. Approximately two hundred returns were displayed, and some were observed to fluctuate from scan-to-scan. Manual data-taking (size and identification) was judged to be inadequate for so large a number of returns. Consequently, the STC curve and threshold were readjusted to display targets of 10^4 m^2 or greater. Twenty-seven discretes were observed to be in this size range, and effort was concentrated on observation and identification of thes discretes. Following this effort, the STC curve and threshold were readjusted for 10^3 m^2 and some limited data taken.

A general view of the clutter is provided by Figures 10 and 11. These PPI photographs, showing raw video, were made with maximum constant receiver gain (no STC applied to receiver). Figures 10 and 11 have radial ranges of 40 and 16 nautical miles, respectively. Blockage to the south from the 30-foot parabolic reflector is clearly defined. The shadowed area to the southwest is primarily due to the proximity of a high hill in that direction; the shadowmap, Figure 9, shows this effect.

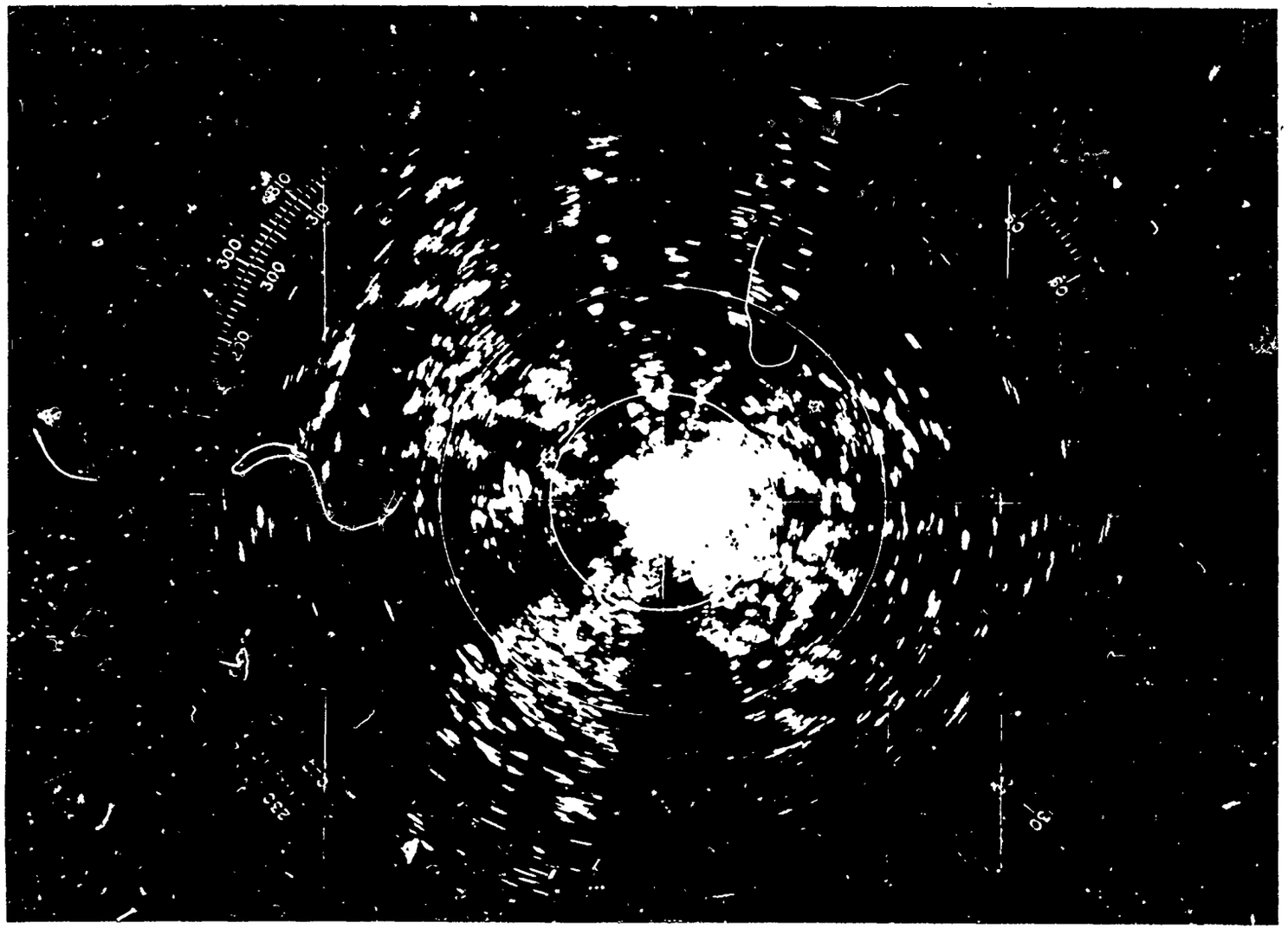

Figure 11 Clutter Map Using Raw Video (16 Mile Radial Range)

B. Discretes $\geq 10^4$ m^2

Over a period of nearly three months, observations were made on twenty-eight discretes approximately equal to or greater than 10^4 m^2. The characteristics of these discretes are described below.

The PPI photographs shown in Figures 12, 13, and 14 are representative of the PPI display as observed over the several-month observation period. All figures have a 16-nautical mile radial range and show thresholded video with STC applied to the receiver; exposure time was 7 scans at an antenna speed of 6 r.p.m. The cross sections displayed are approximately $\geq 10^4$ m^2, $\geq 3 \times 10^4$ m^2, and $\geq 10^5$ m^2, respectively. (Targets #18 and #22 at 23.8 and 27.2 nautical miles, respectively, were observed on the 40-mile PPI display.) Here the use of the 16-mile range permits the display resolution of discretes that are closely spaced in range and/or azimuth. Target #11, though within the maximum range of the display, did not cross the threshold on the day the PPI photograph was taken. A summary of the characteristics of the discretes is given in Table 1. (Target numbers in Table 1 correspond to the numbers shown in Figure 12.) Figure 15 gives the distribution of discretes by cross section.

Observations made of these discretes showed some day-to-day or hour-to-hour "fading" of the smallest discretes, e.g., target #11 as mentioned above. However, these discretes had not

Figure 12 . PPI DISPLAY OF DISCRETES
APPROXIMATELY ≥ 10 m² (16-MILE RADIAL RANGE)

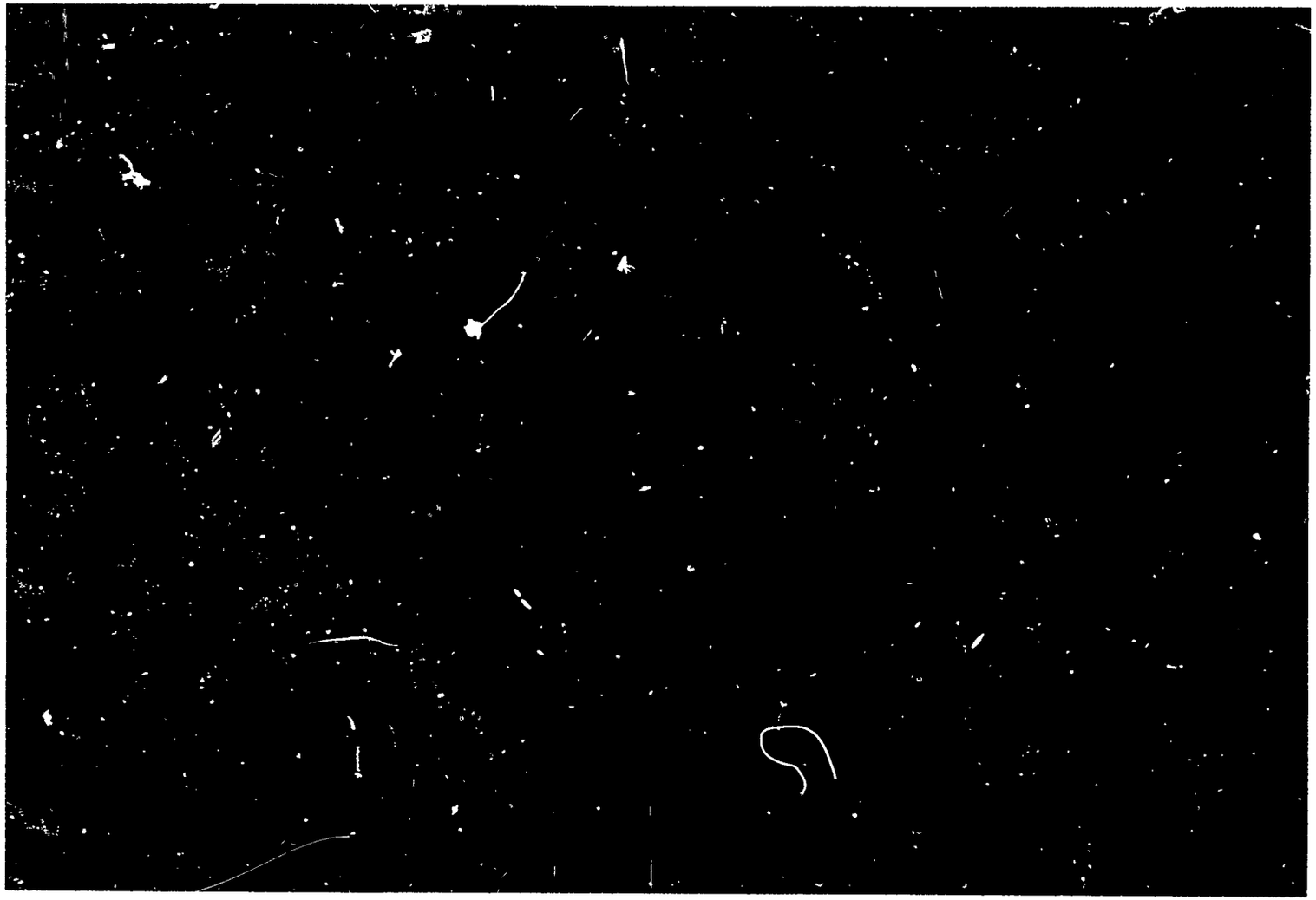

Figure 13 PPI Display of Discretes $\geq 3 \times 10^4$ m^2 (16 Mile Radial Range)

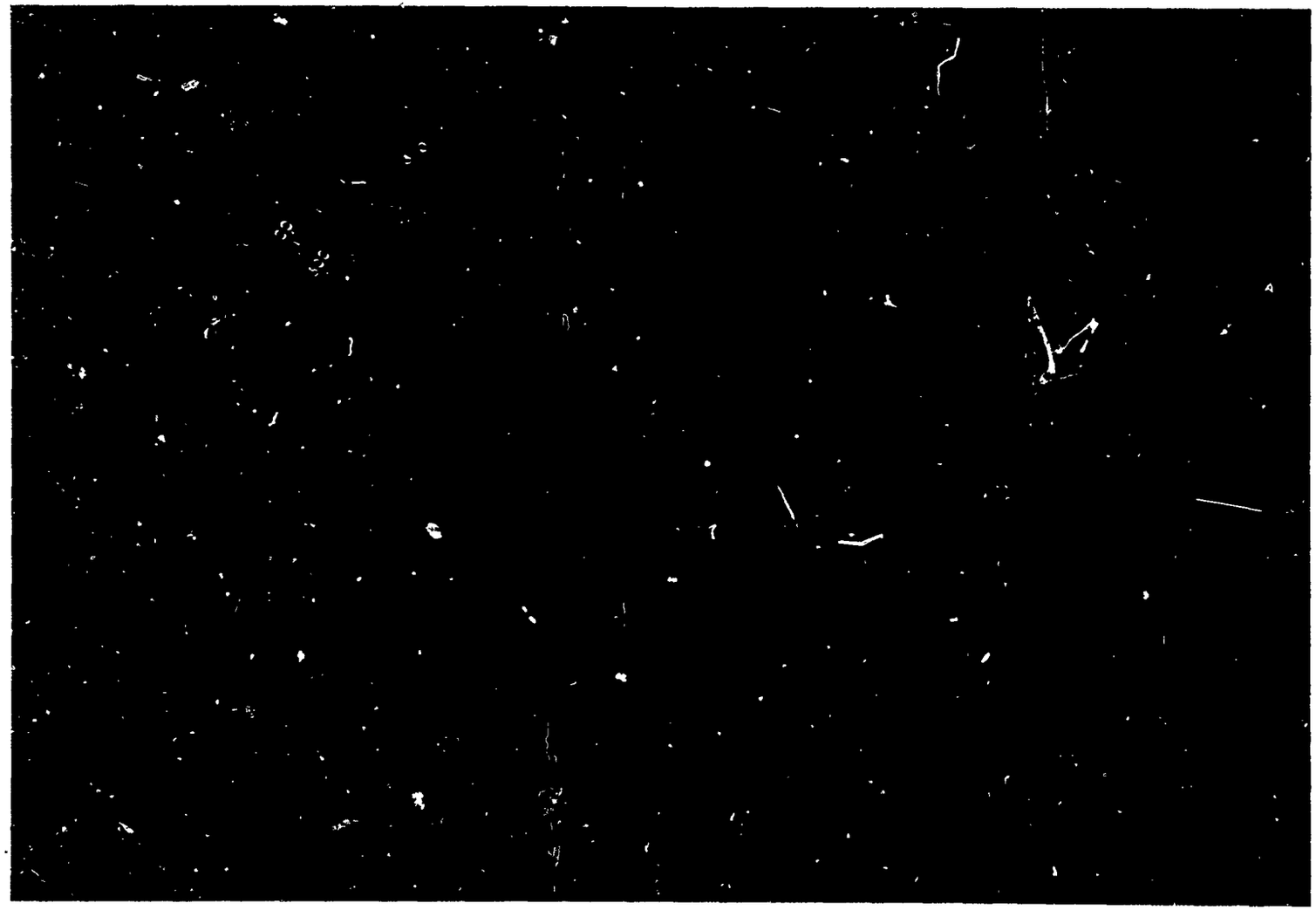

Figure 14 PPI Display of Discretes $\geq 10^5$ m^2 (16 Mile Radial Range)

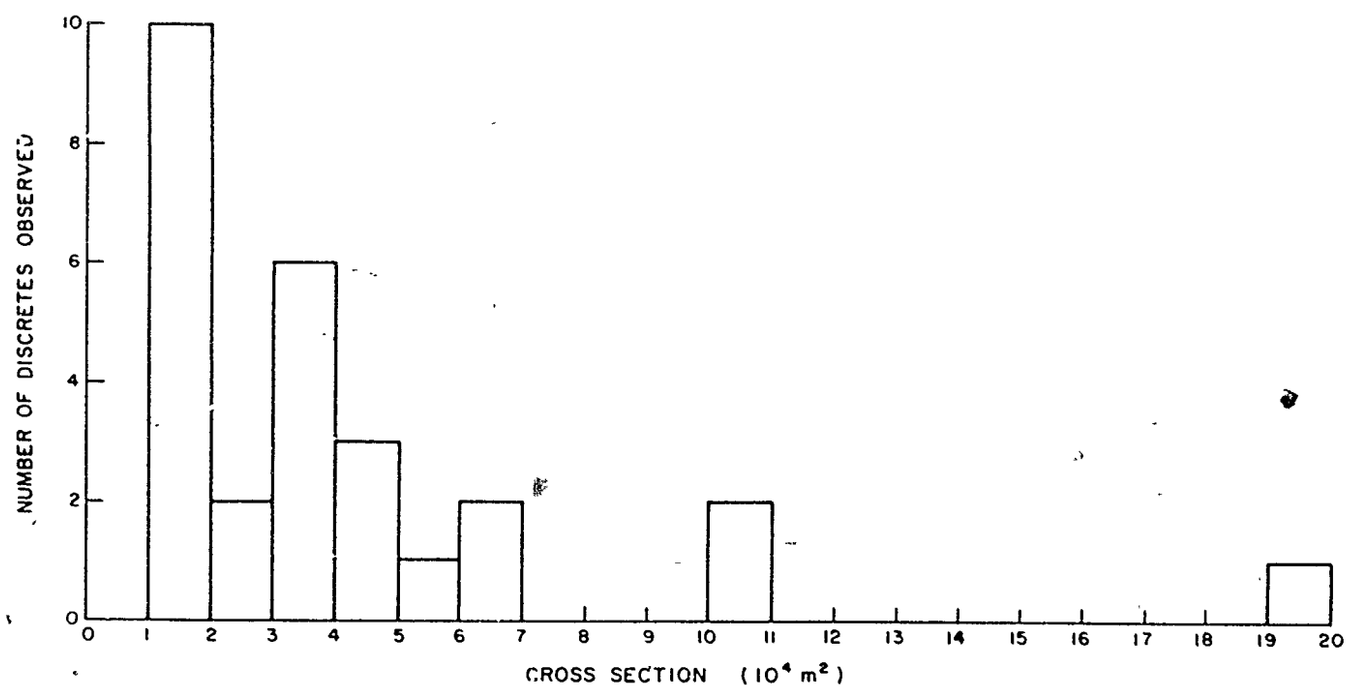

Figure 15. DISTRIBUTION BY CROSS SECTION OF MEASURED DISCRETES ≥ $10^4 m^2$

disappeared entirely, but had diminished to one or two db below that required for thresholding. This is attributed to atmospheric conditions affecting propagation loss, multipath patterns, or both. The cross-section measurements given in Table 1 were made on 4 December 1969, and the PPI photographs of Figures 12, 13, and 14 on 23 October 1969.

An estimate of the fluctuation characteristics of the largest discretes may be gained from A-scope photographs. (All A-scope photographs were taken with one-second exposures.) Figures 16, 17, and 18 are A-scope photographs of targets #2, #3, and #28, and may be regarded as typical. It can be seen that there is no evidence of multiple traces and very little trace thickening due to fluctuation. These discretes are cylindrical water towers, as shown by Figures 19, 20, and 21, which are photographs taken with a camera equipped with a telephoto lens and located at the antenna.

A-scope photographs of two discretes identified as buildings are shown in Figures 22 and 23. Some fluctuation can be observed both preceding and following the discrete returns, most notably in Figure 22. Since these buildings are located at the top or near the top of hills, the fluctuating portions of the returns probably represent that of the hillsides. Observe that in all A-scope photographs the discretes are one pulse width in duration (0.4 μsec).

CHARACTERISTICS OF DISCRETES $\geq 10^4$ m^2

TABLE 1

Target	Range[1]	Azimuth[2]	Cross Section[3]	Description[4]	Elevation[5]	Dimensions[6]	Comments
1	11.3	18	40,960	Water Tower	242		
2	7.5	23	12,600	Water Tower	231	80 x 75	
3	8.95	71.5	67,190	Water Tower	180	80 x 45	
4	6.4	126.5	11,610	Hospital Complex	239		
5	13.1	127.5	17,745	Water Tower	90	100 x 30	
6	13.2	130.5	100,570	Water Tower	90	84 x 40	
7	11.0	134.5	36,775	Water Tower	110	96 x 90	
8	10.1	149.5	45,420	Water Tower	230	40 x 80	
9	7.1	151	8,223	Water Tower	205	48 x 60	(a) Shows ≅ 1.5 db fluctuation; cross section is largest value. (b) Though less than 10^4 m^2, included for sake of completeness.

NOTES:

(1) Range in nautical miles.

(2) Azimuth in degrees relative to true north.

(3) Radar cross section in square meters.

(4) All water towers are cylindrical in shape unless otherwise noted.

(5) Elevation above mean sea level in feet.

(6) All dimensions are approximate values of height times diameter in feet.

TABLE 1 (Continued)

Target	Range	Azimuth	Cross Section	Description	Elevation	Dimensions	Comments
10	10.3	158.5	39,025	Water Tower	180	90 x 30	
11	15.1	174	12,470	See Comments	10	See Comments	(a) A group of oil storage, gasoline and natural gas tanks; the largest is estimated to be 150' x 125'. (b) In presumed shadow of 30' antenna and pedestal. Value of cross section may be low.
12	13.2	195	12,950	Water Tower	370	70 x 40	
13	10.2	197.5	31,220	Water Tower	248	50 x 60	
14	15.0	202	17,150	Water Tower with Supporting legs	315		Large ellipsoid
15	10.8	204	41,080	Water Tower	240	136 x 30	
16	13.7	209	23,815	Two Water Towers, Closely Spaced (≅ 2 feet)	330	90 x 30 90 x 40	
17	10.5	220	50,670	Water Tower	220		
18	23.8	221	64,760	See Comment	602	See Comment	A complex of structures: microwave link, fire tower, 15-foot parabolic antenna on 60-foot tower.
19	11.7	223	31,825	Water Tower	160		Two water towers at almost same range, not resolvable in azimuth. Nearly resolvable in range.
20	11.7	223.5	10,060	Water Tower	160		
21	11.9	223.75	12,090	Two water towers with ≅ 100 ft. separation in azimuth at nearly same range	220		

TABLE 1 (Continued)

Target	Range	Azimuth	Cross Section	Description	Elevation	Dimensions	Comments
22	27.2	227.5	15,785	Water Tower	530	90 x 40	
23	9.3	230	193,280	Water Tower	270	160 x 40	
24	9.3	233.5	108,100	Water Tower	280	120 x 75	
25	10.7	249	21,260	Water Tower	240	96 x 70	
26	12.1	283	16,270	Water Tower	260	72 x 72	
27	6.1	322.5	34,780	Building	120		A seminary or hospital located in a residential section of the city of Lawrence.
28	4.9	356	35,000	Water Tower	255	96 x 40	

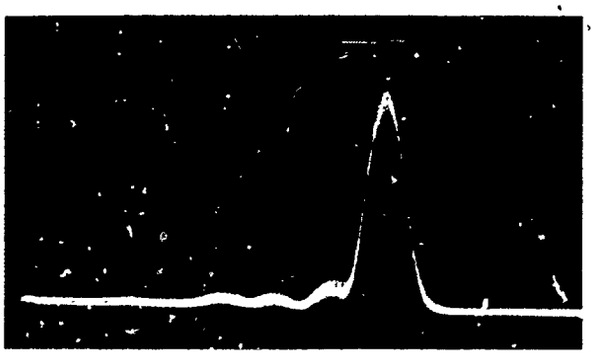

Figure 16. A-SCOPE · PHOTOGRAPH OF TARGET # 2

VERTICAL SCALE : UNCALIBRATED
HORIZONTAL SCALE : 0.5 μ SEC / CM

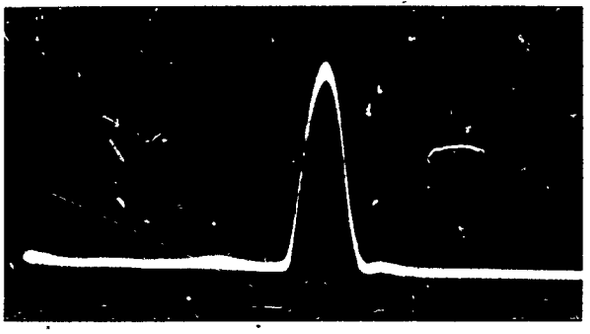

Figure 17. A-SCOPE PHOTOGRAPH OF TARGET # 3

VERTICAL SCALE : UNCALIBRATED
HORIZONTOL SCALE : 0.5 μSEC / CM

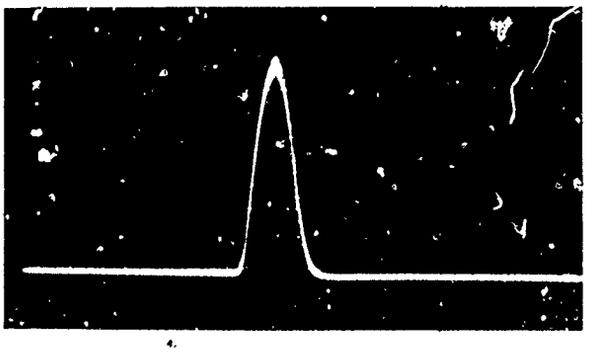

Figure 18 A-SCOPE PHOTOGRAPH OF TARGET # 28

VERTICAL SCALE . UNCALIBRATED
HORIZONTOL SCALE : 0.5μ SEC / CM

Figure 19 View of Target #2

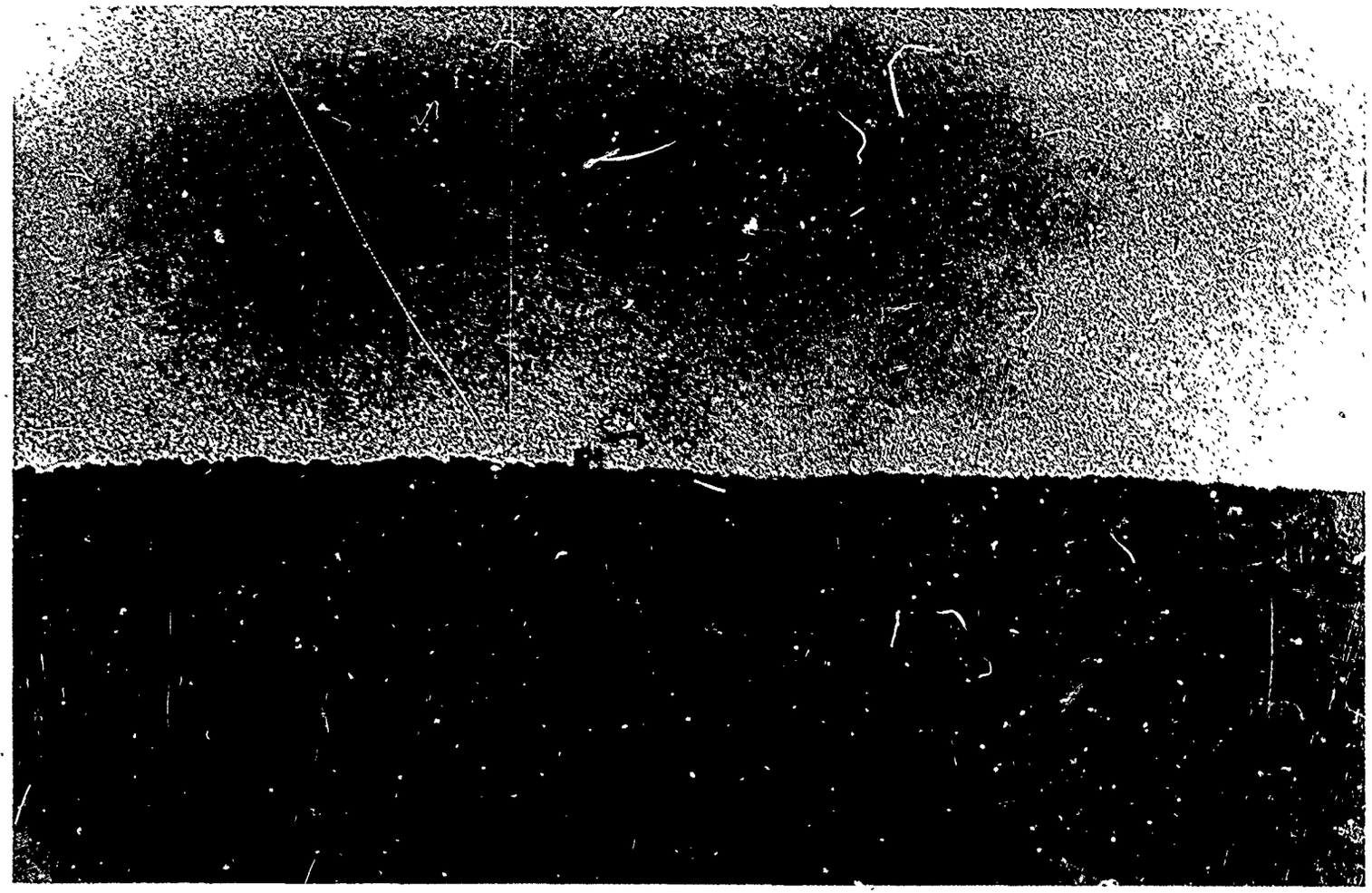

Figure 20 View of Target #3

Figure 21 View of Target #28

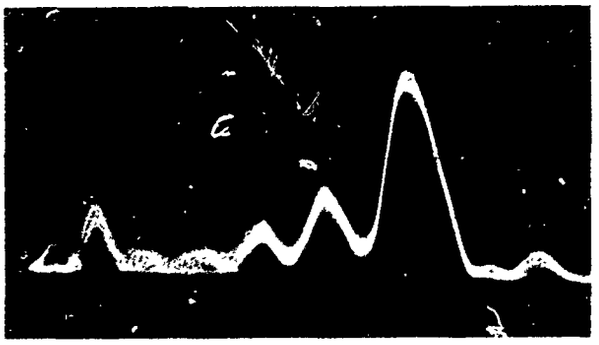

Figure 22. A-SCOPE PHOTOGRAPH OF TARGET #4 (BUILDING COMPLEX AT DANVERS STATE HOSPITAL)

VERTICAL SCALE : UNCALIBRATED
HORIZONTAL SCALE : 0.5 μSEC/CM

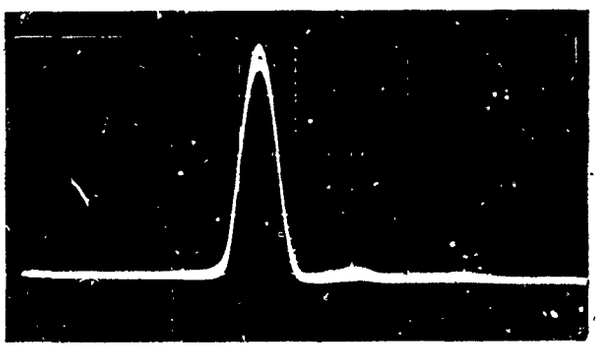

Figure 23. A-SCOPE PHOTOGRAPH OF TARGET #27 (BUILDING IN CITY OF LAWRENCE)

VERTICAL SCALE : UNCALIBRATED
HORIZONTAL SCALE . 0.5 μSEC / CM

Of the twenty-eight discretes identified, twenty-four are cylindrical water towers; two are buildings located at elevations comparable to the radar; and two, though known to be man-made, could not be identified as any single object.

Since water towers are normally situated on hills or ridges, the grazing angle from the Boston-Hill radar to the water towers was extremely small - less than 0.1^{o}, and much less than would be expected from a simple smooth-earth calculation. Maximum radar cross-section for a cylinder (free space, infinite conductivity) occurs for normal illumination. Making allowance for possible multipath effects, off-normal illumination, and imperfect conductivity, there is fair agreement between the calculated and measured cross sections of the observed water towers. In all cases the measured value was less than the calculated.

Comments on some individual discretes are:

(1) Target #9 is approximately 1 db below 10^{4} m^{2} and thresholded due to a deviation of the STC waveform at the corresponding range. It is included, however, since it appears in the PPI photographs.

(2) Target #11 is in the blockage due to the nearby parabolic antenna; the measured cross section is, therefore, suspect. However, if there is significant perturbation of the antenna beam, it seems unlikely that higher equivalent antenna gain would result and more probable that the measured cross section would be greater in the absence of the parabolic reflector.

Investigation of the site where target #11 is located showed several structures too closely spaced to ascertain the exact source of the return. It is believed that the major contribution to the return is from a large natural-gas tank.

(3) Similarly, investigation of the site of target #18 disclosed several structures, and positive identification of the exact source of the return was not possible. It is interesting to note the relatively long range and high elevation associated with this discrete.

(4) The comment made relative to the range and elevation of target #18 also applies to target #22.

(5) Some qualification of the reporting of targets #19 and #20 is appropriate. Figure 24a, b, and c illustrate that #19 and #20 are nearly resolvable in range but not resolvable in azimuth. (In Figure 12, the PPI display, they appear as a single target.) The

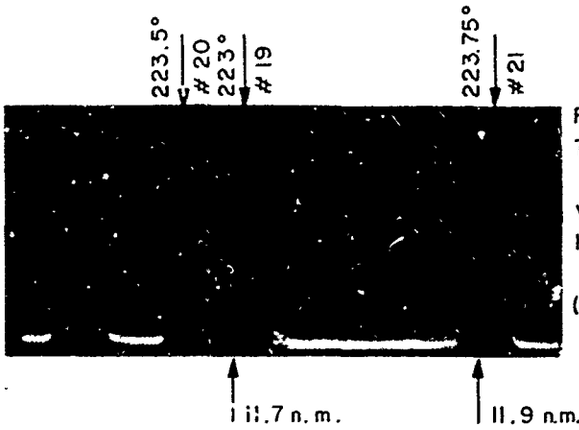

Figure 24. A-SCOPE PHOTOGRAPHS OF TARGETS # 19, # 20 AND # 21

VERTICAL SCALE: UNCALIBRATED
HORIZONTAL SCALE: 0.5 μSEC / CM

(a) ANTENNA PEAKED ON # 19

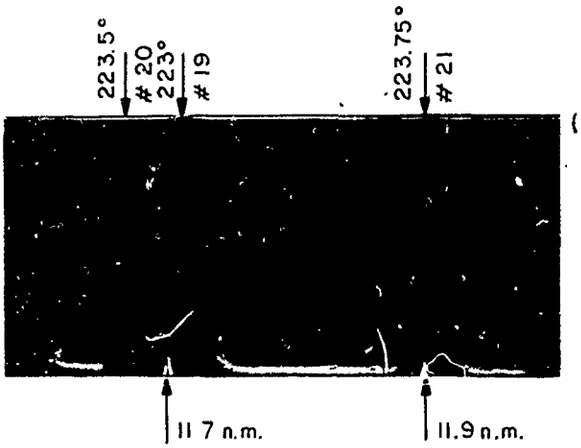

(b) ANTENNA PEAKED ON # 21

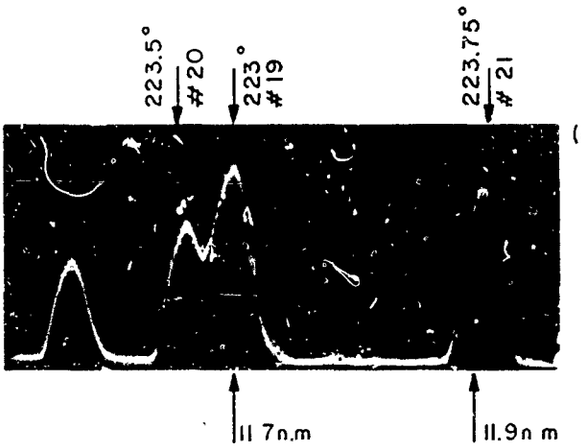

(c) ANTENNA PEAKED ON # 20

values of cross section quoted in Table 1 correspond to the maximum returns associated with each discrete. As such the values are approximate measures of the cross section since the discretes are barely resolvable in range. Similarly, target #21 consists of two small water tanks that are unresolvable in azimuth and range (spacing less than 100 feet).

C. Discretes $\geq 10^3$ m^2

As was discussed earlier, the large number of returns greater than 10^3 m^2 precluded exhaustive investigation of their sources. Nevertheless, some data were taken in the form of PPI photographs, and some limited investigations were made of the discrete sources; these data are presented below.

Figures 25, 26, 27, and 28 are PPI photographs with the threshold level adjusted for 10^3 m^2. In Figure 25, the radial range is 40 n.mi., but the display is blanked beyond 37 n.mi., the maximum range of the STC. Hills are apparent in the west and west-north-west at about 35 miles. Figure 26 is similar to Figure 25 except that the display is blanked beyond 25 miles, the calculated horizon for a smooth earth.

Antenna Scan Rate: 11 r.p.m.
Exposure: 7 scans
(3[illegible] seconds)

Figure 25 PPI Display of Thresholded Video $\geq 10^3$ m^2
Within 37 Miles

Antenna Scan Rate: 11 r.p.m.
Exposure: 7 scans
(38 Seconds)

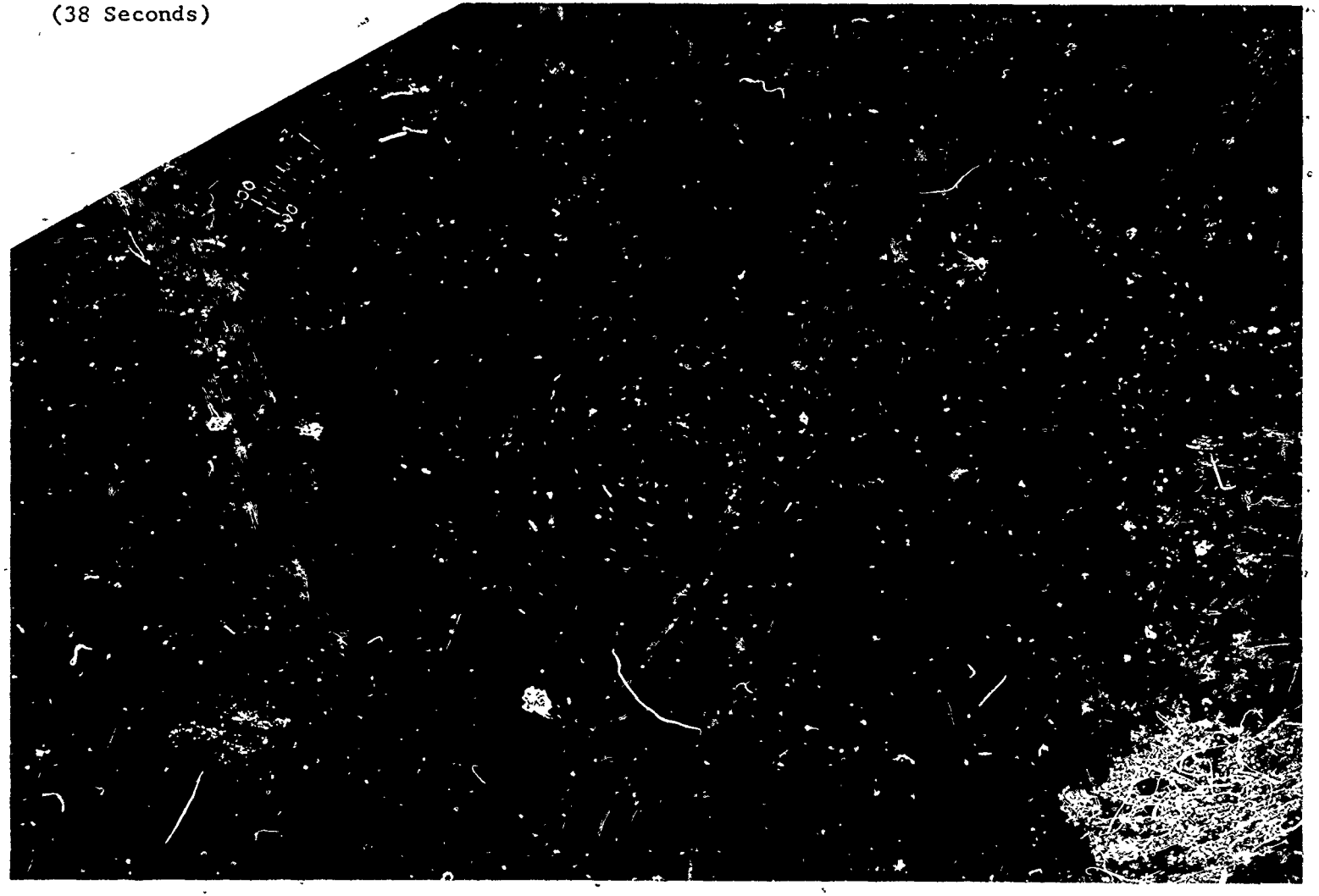

Figure 26 PPI Display of Thresholded Video $\geq 10^{3} m^{2}$ Within 25 Miles

Antenna Scan Rate: 11 r.p.m.
Exposure: 7 Scans
(38 Seconds)

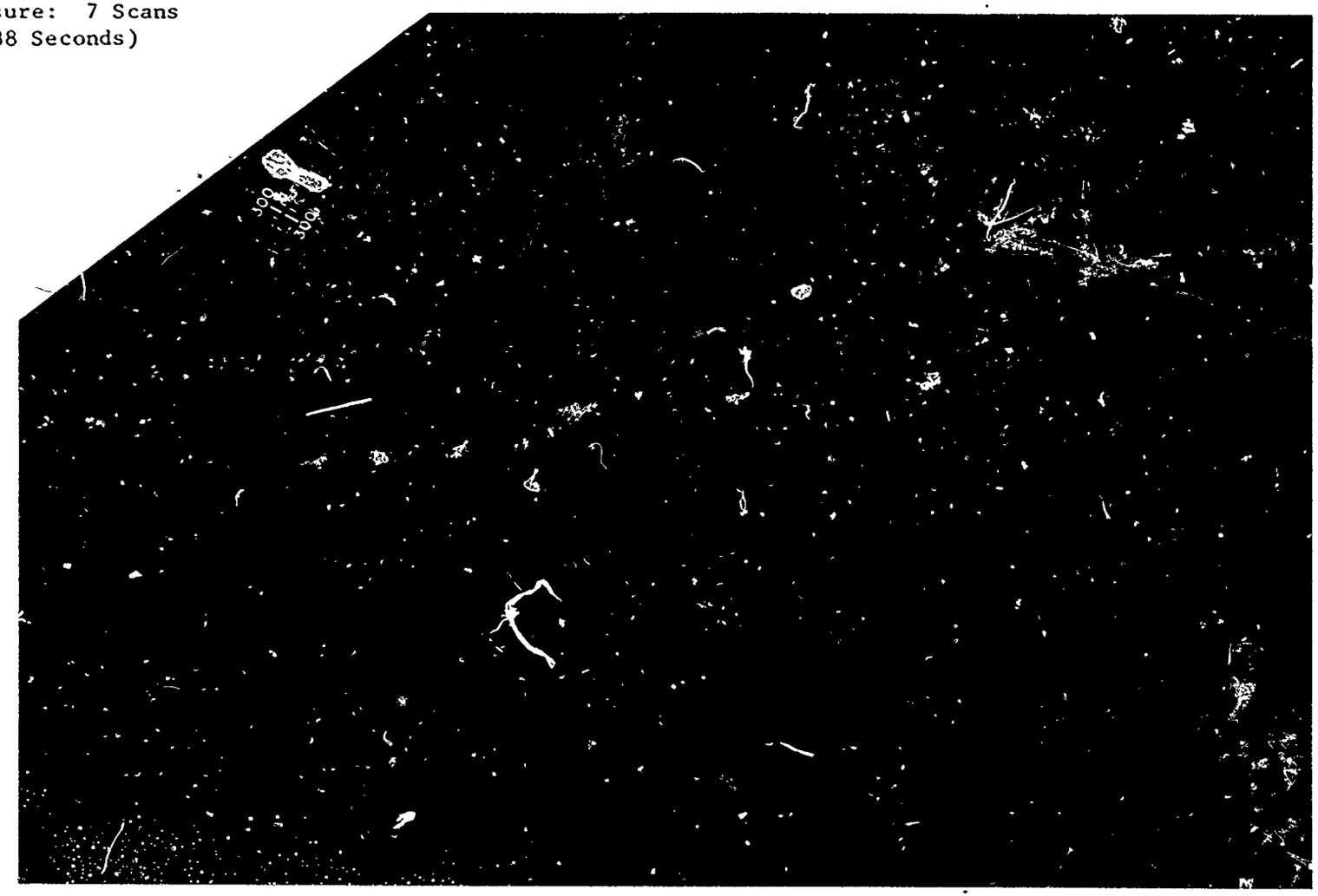

Figure 27 PPI Display of Thresholded Video $\geq 10^3$ m^2 Within 16 Miles

Figure 28 PPI Display of Thresholded Video $\geq 10^3$ m^2 Within 6 Miles

In Figure 27 the radial range is 16 miles, and the display is blanked for the first mile. The photograph records returns which are fluctuating from scan-to-scan, and though not apparent from the photograph, somewhat in excess of 100 returns are displayed consistently from scan-to-scan.

Figure 28 is again similar to the other PPI photographs except that the scale has been expanded to 6 miles.

An examination of some of the returns $\geq 10^3$ m^2 showed that not all returns were from man-made objects. In at least one instance the return was from a hill. This return showed a large fluctuation from sweep-to-sweep, and also from scan-to-scan. In other cases buildings were identified as the sources. Small water towers were observed to cause some returns; these were of a type characterized by a small reservoir mounted on legs. Trucks were identified as the sources of some discrete returns. Portions of Route 114 are aligned radially with respect to Boston Hill (see Figure 7). When this was the case, the returns from some vehicles could be observed to move in range on an A-scope and exceed the threshold.

SECTION V

SUMMARY AND CONCLUSIONS

The observations of discrete returns made from Boston Hill may be summarized as follows:

(1) Twenty-seven discretes were found to have cross sections larger than 10,000 m^2, with the largest being approximately 200,000 m^2. The number of discretes having cross sections larger than 1,000 m^2 is estimated to be in excess of one hundred.

(2) The largest discretes showed little sweep-to-sweep amplitude fluctuation, and were persistent as observed over a period of months. Many of the discretes of less than 10,000 m^2 cross section showed considerable amplitude fluctuation.

(3) All of the discretes larger than 10,000 m^2 were found to be associated with man-made structures having predominant vertical reflecting surfaces; the majority were cylindrical water towers. The nature of man-made objects which give rise to effective cross sections between 1,000 m^2 and 10,000 m^2 appears to be more varied; a cursory examination showed small water towers, vehicles, and buildings to be discrete sources.

(4) Some of the smaller discretes (less than 10,000 m^2) were observed from other than man-made objects, such as small hills.

(5) Using the shadowmap data, which indicate that approximately 20% of the area bounded by the radar horizon was visible from the radar, the density of discretes larger than 10,000 m^2 may be estimated as approximately 0.07 per square mile.

From these observations, we have drawn the following conclusions:

1. "Discretes" do exist at S-band.
2. The larger discretes which have been observed from our particular vantage point at Boston Hill all originate from man-made structures having predominant vertical surfaces. Within our ability to model such specific structures, we can then obtain the three-dimensional re-radiation patterns of these discretes (simply by our now having found out what causes the discrete returns).
3. Within the relatively small range of grazing angles obtained from the Boston Hill vantage point, no large (greater than 10,000 m^2) targets were seen which did not originate from a man-made structure.

b. These extremely small grazing angles (between the water towers and the radar) are to be found only at extreme ranges for the airborne-radar situation. Hence it is probably not valid to extrapolate the areal density as measured to anything like the entire area seen by an airborne radar.

c. These discretes are also seen to be very strongly affected by grazing angle, since they tend to have large vertical apertures and therefore very narrow re-radiating beamwidths in the vertical dimension. Therefore it is evident that they will not be strong reflectors at larger grazing angles (unless some corner-reflector effects are present).

d. Thus, perversely, the experimental results which are most striking and most definite are likely to be least interesting and applicable to airborne radar.

Our recommendations for future experimental work are therefore as follows:

1. Get mobility by using a truck-mounted radar which will provide more azimuthal flexibility, and the ability to obtain a bigger range of grazing angles. The major

It is recognized that the experiments conducted to date suffer from the following weaknesses:

1. It is clear that the experiment is a very "local" affair, in that we are getting a sample of a relatively small (25-mile radius) area; certainly the results are not representative of the entire country or the world.
2. The experiment suffers from a peculiar problem, in that the discretes were necessarily observed at low grazing angles something easily seen after the results of the measurement program were available, but which was not particularly evident before), giving rise to the following:
    a. The particular targets found to be the source of discretes will have their largest cross section at zero grazing angle. But these targets are also very likely (because of their function) to be found at the tops of hills. Thus their grazing angle tends to be a minimum for these targets, and accentuates their strength.

unknown at present is the nature or identification of targets which will have large cross sections at moderately large grazing angles.

2. Get airborne by using a helicopter-lifted radar, which will provide a larger range of grazing angles, and more geographic variety. A helicopter has a number of interesting advantages, among the most important of which is the separation of signal fluctuation due to target changes from those due to platform motion.

REFERENCES

1. Kerr, D. E., "Propagation of Short Radio Waves," Vol. 13 Radiation Laboratory Series, p. 550 et. seq.

2. Lawson, J. L., and Uhlenbeck, G. E., "Threshold Signals," Vol. 24 Radiation Laboratory Series, Chapter 6.

3. Kerr, p. 582.

4. Kerr, p. 354 et seq: p. 361. Figure 4.39 shows the one-way variation in signal for a particular target.

5. Reiss, A., Whitlock, W. S., and Smith, M. H. A., "Land and Precipitation Clutter Measurements at C Band," Fourteenth Annual Tri-Service Radar Symposium, 1968.

6. Edison, A. R., Moore, R. K., and Warner, B. D., "Radar Terrain Return Measured at Near Vertical Incidence," Proceedings of the I.R.E., May 1960, pp. 246-254.

7. Carlson, R., and Greenstein, L., "A Distributed and Discrete Clutter Model for AWACS," Special Technical Report No. 2, AWACS Radar Development Program, June 1969, IIT Research Institute.

8. Carlson et al, p. 21.

9. Hemenway, D. F., Kolnoskas, L. F., and Zuro, S. A., "Final Quarterly Progress Report," 1 April 1967 to 30 June 1967, Naval Research Laboratory, p. 4.

10. Kerr, p. 35, Equation (28).

Security Classification

DOCUMENT CONTROL DATA - R & D

(Security classification of title, body of abstract and indexing annotation must be entered when the overall report is classified)

1 ORIGINATING ACTIVITY (Corporate author) The MITRE Corporation Bedford, Massachusetts	2a. REPORT SECURITY CLASSIFICATION UNCLASSIFIED 2b GROUP

3 REPORT TITLE

Preliminary Report on the Discrete Clutter Measurement Program

4 DESCRIPTIVE NOTES (Type of report and inclusive dates)

N/A

5 AUTHOR(S) (First name, middle initial, last name)

Ellis P. McCurley and William J. McEvoy

6 REPORT DATE	7a TOTAL NO OF PAGES	7b. NO OF REFS
SEPTEMBER 1970	75	10

8a. CONTRACT OR GRANT NO	9a. ORIGINATOR'S REPORT NUMBER(S)
F19 (628)-68-C-0365 b. PROJECT NO 4110 c. d	ESD TR-70-303 9b. OTHER REPORT NO(S) (Any other numbers that may be assigned this report) MTR-1779

10 DISTRIBUTION STATEMENT

This document is subject to special export controls and each transmittal to foreign governments or foreign nationals may be made only with prior approval of Hq. Electronic Systems Division (ESTI).

11 SUPPLEMENTARY NOTES	12 SPONSORING MILITARY ACTIVITY
N/A	Deputy for Airborne Warning and Control Systems, Electronic Systems Division, AF Systems Command, L.G. Hanscom Field, Bedford, Massachusetts

13 ABSTRACT

As part of an experimental investigation of ground clutter being conducted by the MITRE Corporation, data on the magnitudes and distribution of large "discrete" clutter returns have been collected using a radar situated at the Boston Hill field station in North Andover, Massachusetts. Although the experiment is limited in scope and the instrumentation unsophisticated, the measurement program has confirmed some earlier ideas about discrete land clutter, and suggests other promising lines of experimentation. The objectives of this report are to (a) describe the instrumentation, measurement methods, and physical environment, (b) make available the measured results obtained thus far, and (c) provide the background for future effort.

DD FORM 1 NOV 65 1473

Security Classification

Security Classification

14. KEY WORDS	LINK A		LINK B		LINK C	
	ROLE	WT	ROLE	WT	ROLE	WT
RADAR CLUTTER MEASUREMENTS						
DISCRETE CLUTTER						

Security Classification